

Diagrammatic techniques for the nonlinear response of systems dressed by resonant external fields

M. Sanjay Kumar

The Institute of Mathematical Sciences, C.I.T. Campus, Taramani, Madras 600 113, India

G. S. Agarwal

School of Physics, University of Hyderabad, Hyderabad 500 134, India

(Received 13 November 1991)

Diagrammatic methods for the calculation of the nonlinear response of a system that is dressed by resonant external fields are developed. The double-sided diagrams used earlier by Prior [IEEE J. Quantum Electron. **QE-20**, 37 (1984)] for the calculation of nonlinear susceptibilities in the presence of weak fields are generalized. Additional types of double-sided diagrams are given that incorporate explicitly (a) the relaxation-induced population transfers among the dressed levels and (b) the effects of the nonvanishing of the diagonal elements of the dipole operator in the dressed-state basis. The rules for the diagrams are worked out from the analytical structure of the nonlinear response. Applications of the diagrammatic techniques to several intense-field phenomena are discussed.

PACS number(s): 42.50.Hz

I. INTRODUCTION

The presence of a strong pump is known to give rise to many interesting effects in the response of an atomic system to external fields [1–7]. Mollow studied, in a two-level atom, the absorption spectrum of a weak probe in the presence of a strong pump. He showed that a weak probe may be either absorbed or amplified for various probe frequencies in the neighborhood of the frequency of a strong pump [2]. On the other hand, if the probe is scanned around the frequency of transition connecting the excited level to a third level, then an absorption spectrum exhibiting an Autler-Townes doublet is obtained. The resonances at the Rabi frequency of the pump (Rabi splitting) have been shown to occur in a variety of pump-probe experiments [4–7]. Effects such as the above can be described in terms of the response calculated to *all orders* in the strong field but to *first order in the weak fields*. The spectrum of the radiation emitted by a system interacting with a strong pump also exhibits a number of Rabi resonances [1,7].

Further, the absorption and fluorescence signals in a system that is interacting with a strong pump field and a probe field have been found to exhibit resonances at various submultiples of the Rabi frequency of the pump field, as the strength of the probe field is increased [8–10]. Such subharmonic resonances, for example, have been found to be quite important for the understanding of instabilities in laser systems [11] and have been studied experimentally [12]. In addition, the generated radiation in the vicinity of such subharmonic resonances has been shown to exhibit strong squeezing properties [13]. The existence of such subharmonic resonances can be accounted for in terms of the response calculated to *all orders in the strong fields* but to *higher orders in the weak fields* [14]. Recently there has also been considerable interest in the subject of single-photon and multiphoton gain in media pumped by a strong field [15–17]. Such

situations again require response to *all orders in strong fields* but to *different orders* in fields that are to be amplified.

From the above it is clear that in the study of intense-field effects in multilevel systems, one has typically the following situation. The system is interacting with a strong pump field which may be resonant or close to resonance with certain transitions. In addition, the system is interacting with weak fields. Some of these weak fields act as probes of the intense-field dynamics. Here we are interested in the nonlinear response of such a system. Such a nonlinear response can be calculated to, say, *n*th order in the weak fields but it has to be calculated to *all orders in the pump field*. We denote such a nonlinear response by $R^{(n)}$, where the symbol R is used instead of χ to denote the fact that the pump has been treated to all orders. The system could be interacting with more than one pump, with each pump resonant with a different transition [6,7]. Such a nonlinear response and its modifications are useful for describing a large number of phenomena in optical physics, e.g., (1) pump-probe experiments, (2) higher-order-wave mixing, (3) subharmonic Rabi resonances, (4) subharmonic Raman resonances [18,19], (5) fluorescence and ionization from a strongly pumped system, (6) single-photon and multiphoton laser action in systems without population inversion but which are strongly pumped, (7) second-harmonic generation in the presence of dc fields [20,21] and (8) nonlinear optical phenomena in regions where transparency is induced by external fields [22].

In this paper, we show how such a nonlinear response can be calculated for a multilevel system that is undergoing arbitrary relaxation. We work in the dressed-state basis and make use of the dressed-atom approximation [23,25]. We present explicit analytical expressions for $R^{(1)}$, $R^{(2)}$, and $R^{(3)}$. We develop diagrammatic methods to describe each term in the nonlinear response. The rules for the double-sided diagrams are worked out from

the formal structure of the nonlinear response.

The organization of the paper is as follows. In Sec. II we give a brief derivation of the analytical expression for the nonlinear response $R^{(n)}$. In Sec. III we give the explicit analytical result for the linear response $R^{(1)}$. We illustrate the diagrammatic method by calculating the linear response $R^{(1)}$. In Sec. IV we give the explicit analytical result for $R^{(2)}$ and present a diagrammatic calculation of the second-order response. We describe the basic features of the diagrammatic method. From the formal structure of the nonlinear response, we establish the rules for a class of diagrams that depend on the relaxation only of the off-diagonal elements of the density operator in the dressed-state picture. We also introduce a new class of diagrams, namely, the population-transfer diagrams, which are necessary to represent those terms in $R^{(2)}$ (and in general in $R^{(n)}$) which depend on the relaxation-induced population transfers among the various dressed levels. We establish the rules for these diagrams too. We select two typical terms from $R^{(2)}$ and illustrate how the corresponding diagrams may be drawn. In Sec. V we give the explicit analytical result for $R^{(3)}$. We show that there are three classes of diagrams that contribute to $R^{(3)}$ (and in general to $R^{(n)}$). By selecting three typical terms from $R^{(3)}$ we discuss the characteristics of the three classes of diagrams and illustrate how the rules for the two types of diagrams developed in the earlier sections may be used for the drawing of these diagrams. We present the complete diagrammatic calculation of the third-order response. Finally, in Sec. VI we discuss the applications of the diagrammatic techniques developed in the earlier sections to several intense-field phenomena such as subharmonic resonances, dc-field-induced second-harmonic generation, fluorescence and ionization in the presence of a strong pump, etc.

II. ANALYTICAL EXPRESSION FOR THE NONLINEAR RESPONSE TO ALL ORDERS IN STRONG FIELDS

In this section we derive an analytical expression for the nonlinear response to some given order in the weak fields and to all orders in the strong fields. We work in the dressed-state basis and make use of the dressed-state approximation.

A. Density-matrix equation in dressed-state basis

Consider a quantum-mechanical system that is undergoing relaxation and that is interacting with one or more strong fields and with weak fields. The evolution of such a system is described by the dynamical equation [14]

$$\frac{\partial \rho}{\partial t} = -i[H_0 + V(t) + W(t), \rho] + L_R \rho, \quad (2.1)$$

where ρ is the density operator of the system and $V(t)$ [$W(t)$] describes the interaction with the strong [weak] fields. The relaxation of the system is described by the Liouville operator L_R which has the structure

$$(L_R)_{ij} = -\Gamma_{ij}(1 - \delta_{ij})\rho_{ij} + \delta_{ij} \sum_k (\gamma_{ik}\rho_{kk} - \gamma_{ki}\rho_{ii}), \quad (2.2)$$

$$\Gamma_{ij} = \frac{1}{2} \sum_k (\gamma_{ki} + \gamma_{kj}) + \Gamma_{ij}^{\text{ph}}. \quad (2.3)$$

Here Γ_{ij}^{ph} is the rate of dephasing of the coherence ρ_{ij} ($i \neq j$) due to phase-changing collisions, and γ_{ij} gives the rate of transition from state $|j\rangle$ to $|i\rangle$ due to inelastic collisions and spontaneous emission. At this stage we make a canonical transformation with a unitary operator $U(t)$ such that the quantity

$$U^{-1}(t)[H_0 + V(t)]U(t)$$

is time independent. As a result of the canonical transformation, Eq. (2.1) becomes

$$\frac{\partial \bar{\rho}}{\partial t} = -i[\bar{\mathcal{H}}, \bar{\rho}] - i[\bar{W}(t), \bar{\rho}] + L_R \bar{\rho}, \quad (2.4)$$

where

$$\bar{\rho} = U^{-1}(t)\rho U(t), \quad (2.5a)$$

$$\bar{h} = U^{-1}(t)[H_0 + V(t)]U(t) + i\frac{\partial U^{-1}}{\partial t}U, \quad (2.5b)$$

$$\bar{W}(t) = U^{-1}(t)W(t)U(t). \quad (2.5c)$$

It may be noted that such a $U(t)$ can always be chosen provided one neglects the counter-rotating terms in $V(t)$ and provided no two strong fields saturate the same transition. The choice of $U(t)$ will depend on the structure of the energy levels and the external strong fields. Now we make one more canonical transformation $S^{-1}\bar{\rho}S = \tilde{\rho}$, where S is the operator which diagonalizes \bar{h} . The equation of motion for $\tilde{\rho}$ is given by

$$\frac{\partial \tilde{\rho}}{\partial t} = -i[\tilde{\mathcal{H}}, \tilde{\rho}] - i[F(t), \tilde{\rho}] + \mathcal{L}\tilde{\rho}, \quad (2.6)$$

where

$$S^{-1}\bar{h}S = \tilde{\mathcal{H}}, \quad \tilde{\mathcal{H}}|\tilde{i}\rangle = \epsilon_i|\tilde{i}\rangle, \quad (2.7a)$$

$$F(t) = S^{-1}\bar{W}(t)S, \quad (2.7b)$$

$$\mathcal{L}\tilde{\rho} = S^{-1}[L_R(S\tilde{\rho}S^{-1})]S. \quad (2.7c)$$

Here, $|\tilde{i}\rangle$ denote the dressed states of the system with energies given by ϵ_i . These are the eigenstates of the combined atom and strong-field Hamiltonian [23]. The operator $F(t)$ represents the interaction of the weak fields with the strong-field-dressed system. It may be noted that if one makes the rotating-wave approximation with respect to the weak fields, then, as a result of the canonical transformations, the rapid oscillations at the optical frequencies in the weak-field interaction $F(t)$ are removed. Thus the new interaction $F(t)$ has only slowly oscillating components. The Liouville operator \mathcal{L} represents the relaxation of the strong-field-dressed system. We now make the secular approximation [23–25] (which is generally valid for strong fields) so that \mathcal{L} can be approximated by

$$(\mathcal{L}\tilde{\rho})_{ij} \approx -q_{ij}(1 - \delta_{ij})\tilde{\rho}_{ij} + \delta_{ij} \sum_k (p_{ik}\tilde{\rho}_{kk} - p_{ki}\tilde{\rho}_{ii}). \quad (2.8)$$

Here q_{ij} is the decay rate of the off-diagonal element of the density operator in the dressed-state picture, namely,

$\tilde{\rho}_{ij}$, whereas p_{ij} denotes the rate of decay of the dressed state $|\tilde{j}\rangle$ to $|\tilde{i}\rangle$. It may be noted that in general for an operator A , \tilde{A}_{ij} may be defined either as $\langle i|\tilde{A}|j\rangle$ or as $\langle \tilde{i}|A|\tilde{j}\rangle$, the two definitions being equivalent. In the first definition the operator is transformed to the new picture while the basis is the old one, whereas the reverse is true in the second definition. The decay rates q_{ij} and p_{ij} depend, through the elements of the transformation matrix S , on the Rabi frequencies of the pump fields. It may be noted that both the downward as well as the upward transitions among the dressed states are important since, in general, p_{ij} is nonzero whether $\varepsilon_i > \varepsilon_j$ or vice versa. This is in contrast to the case when the pump is absent, where the rate of transition from $|j\rangle$ to $|i\rangle$, namely, γ_{ij} , is nonzero only if $E_j > E_i$ (corresponding to the case of spontaneous emission), unless the system undergoes inelastic collisions. If the pump is weak, the transition rates p_{ij} depend linearly on the pump intensity. However, if the pump is strong, then the dependence of p_{ij} on the pump intensity is quite complicated in general.

B. Response functions to different orders in weak fields

The nonlinear response is related to the induced polarization $P(t)$ which can be calculated to n th order in the weak fields from the relation

$$P^{(n)}(t) = \text{Tr}[\mathbf{d}\rho^{(n)}(t)] . \quad (2.9)$$

In terms of the density operator in the dressed-state picture $\tilde{\rho}^{(n)}(t)$, the μ th component of the n th-order induced polarization can be written as

$$P_\mu^{(n)}(t) = \text{Tr}[\tilde{d}^\mu(t)\tilde{\rho}^{(n)}(t)] , \quad (2.10)$$

$$\tilde{d}^\mu(t) = S^{-1}U^{-1}(t)d^\mu U(t)S , \quad (2.11)$$

where d^μ is the μ th component of the dipole-moment operator \mathbf{d} , and $\tilde{\rho}^{(n)}(t)$ is computed from Eq. (2.6). In view of the definition (2.11), one can expand $\tilde{d}^\mu(t)$ in the form

$$\tilde{d}^\mu(t) = \sum_q \tilde{d}_q^\mu e^{-i\omega_q t} , \quad (2.12)$$

where ω_q can be either positive or negative. The modified interaction $F(t)$ [Eq. (2.7b)] can then be expressed as

$$F(t) = - \sum_\alpha \tilde{d}^\alpha(t)E_\alpha(t) , \quad (2.13)$$

which in terms of the Fourier transform of the weak field $\mathbf{E}(t)$ and in view of the expansion (2.12) can be cast in the simple form

$$F(t) = - \sum_{\alpha,a} \tilde{d}_a^\alpha \left[\frac{1}{2\pi} \right] \int_{-\infty}^{\infty} d\omega e^{-i(\omega+\omega_a)t} E_\alpha(\omega) . \quad (2.14)$$

It may be noted that the upper (Greek) index in \tilde{d}_a^α corresponds to the Cartesian component of the vector \mathbf{d} whereas the lower (Latin) index corresponds to a particular Fourier component in the expansion (2.12). It is clear from Eq. (2.14) that the Fourier components of the new interaction $F(t)$ consist of combinations of the weak-field and the strong-field frequencies as a result of the transformation to the dressed-state representation.

By using the decompositions (2.12) and (2.14) one can now express $P_\mu^{(n)}(t)$ in terms of the nonlinear response $R^{(n)}$ in the following manner [14]:

$$P_\mu^{(n)}(t) = \sum_{q\{\alpha_n\}} \sum_{\mu\{\alpha_n\}} \left[\frac{1}{2\pi} \right]^n \int_{-\infty}^{\infty} d\omega_1 \cdots \int_{-\infty}^{\infty} d\omega_n \exp \left[-i\omega_q t - it \sum_{i=1}^n \Omega_i \right] \times R_{\mu\{\alpha_n\}}^{(n)}(\omega_q, \{\Omega_n\}) E_{\alpha_1}(\omega_1) \cdots E_{\alpha_n}(\omega_n) , \quad (2.15)$$

where $R^{(n)}$ is given by the expression

$$R_{\mu\{\alpha_n\}}^{(n)}(\omega_q, \{\Omega_n\}) = \frac{N}{n!} \text{Tr} \left\{ \tilde{d}_q^\mu \left[iL_0 - \sum_{i=1}^n \Omega_i \right]^{-1} L_{\alpha_1 a_1} \left[iL_0 - \sum_{i=2}^n \Omega_i \right]^{-1} L_{\alpha_2 a_2} \cdots (iL_0 - \Omega_n)^{-1} L_{\alpha_n a_n} \tilde{\rho}^{(0)} \right\}_{\text{sym}} , \quad (2.16)$$

$$L_0 \equiv i[\mathcal{H},] + \mathcal{L} , \quad (2.17)$$

$$L_{aa} \equiv -i[\tilde{d}_a^\alpha,] . \quad (2.18)$$

Here we have defined Ω_i to stand for the sum of frequencies $\omega_i + \omega_{a_i}$, where ω_i is a Fourier component of the weak field $\mathbf{E}(t)$ whereas ω_{a_i} is a Fourier component of the dipole-moment operator in the dressed-state picture appearing in the expansion (2.12). For instance, in the simple case when there is only one pump ω_l and one probe

ω_s , one can choose a transformation $U(t)$ such that ω_q can take values $\pm\omega_l$ and hence the Ω_i 's can assume values $\pm(\omega_s - \omega_l)$. The density operator $\tilde{\rho}^{(0)}$ describes the steady state of the dressed atom and hence is subject to the restriction $\tilde{\rho}_{ij}^{(0)} = \tilde{\rho}_{ii}^{(0)}\delta_{ij}$. The quantity N represents the number density of the atoms. The sub-

script ‘‘sym’’ in Eq. (2.16) implies that the quantity in the curly brackets has to be symmetrized with respect to the pairs of indices (Ω_i, α_i) , $i = 1, 2, \dots, n$. It may be noted that $R^{(n)}$ as given by the expression (2.16) appears as the coefficient of the term oscillating with the frequency $\omega_q + \sum_{i=1}^n \Omega_i$ in the Fourier expansion of $P_\mu^{(n)}(t)$ [Eq. (2.15)]. Hence the nonlinear response $R_{\mu\{\alpha_n\}}^{(n)}(\omega_q, \{\Omega_n\})$ describes the generation of radiation with the frequency $\omega_q + \sum_{i=1}^n \Omega_i = \omega_q + \sum_{i=1}^n (\omega_i + \omega_{a_i})$.

C. Expectation values of the atomic observables

The above formulation enables us to compute not only the induced polarization but also the expectation values of the system observables, for example, the atomic level

$$N_i = \sum_{\{\alpha_n\}} \sum_{\{a_n\}} \left[\frac{1}{2\pi} \right]^n \int_{-\infty}^{\infty} d\omega_1 \cdots \int_{-\infty}^{\infty} d\omega_n \exp \left[-it \sum_{i=1}^n \Omega_i \right] \mathcal{N}_{i\{\alpha_n\}}^{(n)}(\{\Omega_n\}) E_{\alpha_1}(\omega_1) \cdots E_{\alpha_n}(\omega_n), \quad (2.20)$$

where the quantity $\mathcal{N}_{i\{\alpha_n\}}^{(n)}(\{\Omega_n\})$ is obtained from the n th-order response $R_{\mu\{\alpha_n\}}^{(n)}(\omega_q, \{\Omega_n\})$ [Eq. (2.16)] by putting $\omega_q = 0$ and replacing \tilde{d}_q^μ by the operator $S^{-1}|i\rangle\langle i|S$.

D. Eigenfunctions and eigenvalues of the Liouville operator

In order to obtain explicit expressions for $R^{(n)}$ to some given order n , we need to know the eigenvalues and eigenfunctions of the Liouville operator L_0 . It follows from Eq. (2.17) that $|\tilde{i}\rangle\langle\tilde{j}|$ ($i \neq j$) form a set of eigenfunctions of L_0 . Thus

$$L_0|\tilde{i}\rangle\langle\tilde{j}| = -i\Lambda_{ij}|\tilde{i}\rangle\langle\tilde{j}|, \quad (2.21a)$$

$$\Lambda_{ij} = \varepsilon_i - \varepsilon_j - iq_{ij}, \quad i \neq j. \quad (2.21b)$$

Another set of eigenfunctions of L_0 can be constructed in terms of the diagonal basis vectors $|\tilde{i}\rangle\langle\tilde{i}|$. It may be noted that L_0 is not diagonal in this basis, since

$$L_0|\tilde{i}\rangle\langle\tilde{i}| = \sum_j D_{ji}|\tilde{j}\rangle\langle\tilde{j}|, \quad (2.22)$$

where D is the population relaxation matrix defined by

$$D_{ij} = p_{ij} (i \neq j), \quad D_{ii} = -\sum_j p_{ji}. \quad (2.23)$$

The eigenvalues and eigenfunctions of L_0 in this basis can be obtained by solving the eigenvalue problem for the population relaxation matrix D . Thus if we write

$$L_0\phi_k = \lambda_k\phi_k, \quad (2.24)$$

then, the eigenfunctions ϕ_k are given by

$$\phi_k = \sum_j A_{jk}|\tilde{j}\rangle\langle\tilde{j}|, \quad |\tilde{j}\rangle\langle\tilde{j}| = \sum_k (A^{-1})_{kj}\phi_k, \quad (2.25)$$

where A is the matrix that diagonalizes D , i.e., $A^{-1}DA = \lambda$, where $\lambda_{ij} = \lambda_i\delta_{ij}$. Having gotten the eigenvalues and eigenfunctions of L_0 , one can obtain the ac-

populations. A knowledge of the level populations is important in the study of the fluorescence and ionization signals in the presence of strong pump fields and weak probe fields. The population N_i of the state $|i\rangle$ will be given by

$$\begin{aligned} N_i &= \text{Tr}[|i\rangle\langle i|\rho(t)] \\ &= \text{Tr}[S^{-1}U^{-1}(t)|i\rangle\langle i|U(t)S\bar{\rho}(t)], \end{aligned} \quad (2.19)$$

where U and S are the matrices (as explained above) that transform the bare-atom quantities to the dressed-atom picture. Usually the diagonal operator $|i\rangle\langle i|$ is left unchanged by $U(t)$. Thus the population of the level $|i\rangle$ to some n th order in the weak field but to all orders in the strong field will be given by

tion of any arbitrary function $f(L_0)$ on any arbitrary operator Q . Thus we have

$$\begin{aligned} f(L_0)Q &= \sum_{k,j} Q_{kj} f(-i\Lambda_{kj})|\tilde{k}\rangle\langle\tilde{j}|(1-\delta_{kj}) \\ &\quad + \sum_{k,m,n} Q_{kk} (A^{-1})_{nk} f(\lambda_n) A_{mn}|\tilde{m}\rangle\langle\tilde{m}|. \end{aligned} \quad (2.26)$$

In particular, we have the following relation which is quite useful in simplifying the expression in Eq. (2.16):

$$\begin{aligned} (iL_0 - \Omega)^{-1}|\tilde{i}\rangle\langle\tilde{j}| &= (\Lambda_{ij} - \Omega)^{-1}(1-\delta_{ij})|\tilde{i}\rangle\langle\tilde{j}| \\ &\quad + \delta_{ij} \sum_k B_{ik}(\Omega)|\tilde{k}\rangle\langle\tilde{k}|, \end{aligned} \quad (2.27)$$

where we have defined

$$B_{ik}(\Omega) = \sum_n (A^{-1})_{ni} A_{kn} (i\lambda_n - \Omega)^{-1}. \quad (2.28)$$

The physical meaning of the B terms can be understood, for instance, by considering the case when there are no weak fields. In this case, the populations of the dressed levels at two different times obey the relation

$$\tilde{\rho}_{ii}(t) = \sum_k \mathcal{P}_{ik}(t)\tilde{\rho}_{kk}(0), \quad (2.29)$$

$$\mathcal{P}(t) = e^{Dt}, \quad t > 0, \quad (2.30)$$

where D is the population-relaxation matrix defined by Eq. (2.23). It may be noted that $\mathcal{P}_{ik}(t)$ in Eq. (2.29) corresponds to the probability that the system is in the dressed state $|\tilde{i}\rangle$ at time t given that it was in the dressed state $|\tilde{k}\rangle$ at time $t=0$. The quantity $B_{ik}(\Omega)$ defined by Eq. (2.28) is related to the Laplace transform of the conditional probability $\mathcal{P}_{ki}(t)$ in the following manner:

$$B_{ik}(\Omega) = i \int_0^\infty dt e^{i\Omega t} \mathcal{P}_{ki}(t). \quad (2.31)$$

Hence it follows that $B_{ik}(\Omega)$ refers to a population transfer from dressed state $|\tilde{i}\rangle$ to $|\tilde{k}\rangle$ due to the relaxation processes in the presence of strong pumps.

III. LINEAR RESPONSE

It follows from Eq. (2.15) that the induced polarization to first order in the weak fields and to all orders in the strong fields is related to the linear response $R^{(1)}$ in the following manner:

$$P_{\mu}^{(1)}(t) = \sum_{\alpha, q, a} \left[\frac{1}{2\pi} \right] \int_{-\infty}^{\infty} d\omega e^{-i(\omega_q + \Omega)t} \times R_{\mu\alpha}^{(1)}(\omega_q, \Omega) E_{\alpha}(\omega), \quad (3.1)$$

where Ω stands for the sum $\omega + \omega_a$, with ω being a Fourier component of the weak field and ω_a a Fourier component in $\tilde{d}^{\alpha}(t)$ [Eq. (2.12)]. The general expression for the linear response follows from Eq. (2.15) and is given by

$$R_{\mu\alpha}^{(1)}(\omega_q, \Omega) = N \text{Tr}[\tilde{d}_{\mu}^{\alpha}(iL_0 - \Omega)^{-1} L_{\alpha\alpha} \tilde{\rho}^{(0)}]. \quad (3.2)$$

In order to simplify the expression (3.2), we write

$$\tilde{\rho}^{(0)} = \sum_i \tilde{\rho}_{ii}^{(0)} |\tilde{i}\rangle \langle \tilde{i}|, \quad (3.3)$$

and make use of the result (2.27). This leads to the result

$$R_{\mu\alpha}^{(1)}(\omega_q, \Omega) = N \sum_{i,j} \tilde{\rho}_{ii}^{(0)} [(\tilde{d}_{\alpha}^{\alpha})_{ji} (\tilde{d}_{\mu}^{\mu})_{ij} (\Lambda_{ji} - \Omega)^{-1} + (-\tilde{d}_{\alpha}^{\alpha})_{ij} (\tilde{d}_{\mu}^{\mu})_{ji} (\Lambda_{ij} - \Omega)^{-1}]. \quad (3.4)$$

It is important to bear in mind that the lower indices q and a in $R_{\mu\alpha}^{(1)}(\omega_q, \Omega)$ ($\Omega = \omega + \omega_a$) relate to the Fourier components ω_q and ω_a appearing in the expansions, respectively, of $\tilde{d}^{\mu}(t)$ and $\tilde{d}^{\alpha}(t)$ [Eq. (2.12)].

In Eq. (3.1), $R_{\mu\alpha}^{(1)}(\omega_q, \Omega)$ is the coefficient of the term in the Fourier expansion of $P_{\mu}^{(1)}(t)$ that is oscillating with the frequency $\omega_q + \Omega$. Thus $R_{\mu\alpha}^{(1)}(\omega_q, \Omega)$ describes the generation of radiation with frequency $\omega_q + \Omega$. It can be seen from Eq. (3.4) that *resonances in the linear response occur when a combination of the strong-field and weak-field frequencies $\Omega (= \omega_a + \omega)$ becomes equal to one of the transition frequencies of the dressed atom*. It may be noted that the linear response is determined only by the relaxation of the off-diagonal elements of the density matrix.

Consider for simplicity the case in which the system is interacting with one pump (ω_l) and one probe (ω_s). In this case, as we have noted before, ω_q and Ω can, respectively, take the values $\pm(\omega_s - \omega_l)$ and $\pm(\omega_s + \omega_l)$. Hence $P_{\mu}^{(1)}(t)$ can be expressed in the form

$$P_{\mu}^{(1)}(t) = e^{-i\omega_s t} R_{\text{abs}}^{(1)} \mathcal{E}_s + e^{-i(2\omega_l - \omega_s)t} R_{\text{FWM}}^{(1)} \mathcal{E}_s^* + \text{H.c.} + (\text{other terms}), \quad (3.5)$$

where $R_{\text{abs}}^{(1)}$ and $R_{\text{FWM}}^{(1)}$ describe, respectively, the absorption of energy from the probe ω_s in the presence of the pump ω_l and the generation of radiation with frequency $2\omega_l - \omega_s$ (four-wave mixing). We find that the quantities $R_{\text{abs}}^{(1)}$ and $R_{\text{FWM}}^{(1)}$ are explicitly given by

$$R_{\text{abs}}^{(1)} = R_{\mu\alpha}^{(1)}(\omega_l, \delta) = N \sum_{\alpha} \sum_{i,j} (\tilde{\rho}_{ii}^{(0)} - \tilde{\rho}_{jj}^{(0)}) (\tilde{d}_{-}^{\alpha})_{ji} \times (\tilde{d}_{+}^{\mu})_{ij} (\Lambda_{ji} - \delta)^{-1}, \quad (3.6a)$$

$$R_{\text{FWM}}^{(1)} = R_{\mu\alpha}^{(1)}(\omega_l, -\delta) = N \sum_{\alpha} \sum_{i,j} (\tilde{\rho}_{ii}^{(0)} - \tilde{\rho}_{jj}^{(0)}) (\tilde{d}_{+}^{\alpha})_{ji} \times (\tilde{d}_{+}^{\mu})_{ij} (\Lambda_{ji} + \delta)^{-1}, \quad (3.6b)$$

$$\delta = (\omega_s - \omega_l). \quad (3.6c)$$

Here \tilde{d}_{+} and \tilde{d}_{-} are the coefficients of the positive and negative frequency terms in the expansion of $\tilde{d}(t)$,

$$\tilde{d}(t) = \tilde{d}_{+} e^{-i\omega_l t} + \tilde{d}_{-} e^{i\omega_l t}. \quad (3.7)$$

The quantities $R_{\text{abs}}^{(1)}$ and $R_{\text{FWM}}^{(1)}$ have been used in the literature in studying a wide variety of phenomena arising in the presence of a strong pump and a weak probe [2-5].

It may be noted that the "other terms" in Eq. (3.5) arise due to the counter-rotating terms in the weak-field interaction $W(t)$ in the bare-atom picture and hence correspond to nonresonant processes, namely, a nonresonant contribution to the absorption at the probe frequency and the generation of radiation at the frequency $2\omega_l + \omega_s$. It may be noted that the pump (dressing) field was treated under the rotating-wave approximation. This was inevitable since otherwise it would not have been possible to transform away the time dependence in the atom-pump interaction $V(t)$. However, one can use the linear response $R^{(1)}$ to take into account the effects of the counter-rotating terms by treating such terms to first order.

IV. DIAGRAMMATIC CALCULATION OF SECOND-ORDER RESPONSE

Before we proceed to present the diagrammatic calculation of the second-order response $R^{(2)}$, we give below the analytical result for $R^{(2)}$ which follows from the general result Eq. (2.16):

$$R_{\mu\alpha\beta}^{(2)}(\omega_q, \Omega_1, \Omega_2) = \frac{N}{2!} [A_{\mu\alpha\beta}^{(2)}(\omega_q, \Omega_1, \Omega_2) + B_{\mu\alpha\beta}^{(2)}(\omega_q, \Omega_1, \Omega_2)], \quad (4.1)$$

where $A^{(2)}$ and $B^{(2)}$ are given by the expressions

$$A_{\mu\alpha\beta}^{(2)}(\omega_q, \Omega_1, \Omega_2) = \sum_{ijk} \tilde{\rho}_{ii}^{(0)} \left[\frac{(\tilde{d}_q^\mu)_{ik} (\tilde{d}_a^\alpha)_{kj} (\tilde{d}_b^\beta)_{ji}}{(\Lambda_{ji} - \Omega_2)(\Lambda_{ki} - \Omega_1 - \Omega_2)} + \frac{(-\tilde{d}_b^\beta)_{ik} (-\tilde{d}_a^\alpha)_{kj} (\tilde{d}_q^\mu)_{ji}}{(\Lambda_{ik} - \Omega_2)(\Lambda_{ij} - \Omega_1 - \Omega_2)} \right. \\ \left. + \frac{(-\tilde{d}_a^\alpha)_{ik} (\tilde{d}_q^\mu)_{kj} (\tilde{d}_b^\beta)_{ji}}{(\Lambda_{ji} - \Omega_2)(\Lambda_{jk} - \Omega_1 - \Omega_2)} + \frac{(-\tilde{d}_b^\beta)_{ik} (\tilde{d}_q^\mu)_{kj} (\tilde{d}_a^\alpha)_{ji}}{(\Lambda_{ik} - \Omega_2)(\Lambda_{jk} - \Omega_1 - \Omega_2)} \right] + \dots, \quad (4.2)$$

where the ellipsis denotes terms obtained by interchanging $(\Omega_1, \alpha) \leftrightarrow (\Omega_2, \beta)$, and

$$B_{\mu\alpha\beta}^{(2)}(\omega_q, \Omega_1, \Omega_2) = \sum_{ijk} \tilde{\rho}_{ii}^{(0)} \left[\frac{(\tilde{d}_q^\mu)_{jj} (\tilde{d}_a^\alpha)_{ik} (\tilde{d}_b^\beta)_{ki}}{(\Lambda_{ki} - \Omega_2)} B_{ij}(\Omega_1 + \Omega_2) + \frac{(-\tilde{d}_b^\beta)_{ik} (-\tilde{d}_a^\alpha)_{ki} (\tilde{d}_q^\mu)_{jj}}{(\Lambda_{ik} - \Omega_2)} B_{ij}(\Omega_1 + \Omega_2) \right. \\ \left. + \frac{(-\tilde{d}_a^\alpha)_{ik} (\tilde{d}_q^\mu)_{jj} (\tilde{d}_b^\beta)_{ki}}{(\Lambda_{ki} - \Omega_2)} B_{kj}(\Omega_1 + \Omega_2) + \frac{(-\tilde{d}_b^\beta)_{ik} (\tilde{d}_q^\mu)_{jj} (\tilde{d}_a^\alpha)_{ki}}{(\Lambda_{ik} - \Omega_2)} B_{kj}(\Omega_1 + \Omega_2) \right] + \dots \quad (4.3)$$

where again the ellipsis denotes terms obtained by interchanging $(\Omega_1, \alpha) \leftrightarrow (\Omega_2, \beta)$.

In writing the expressions (4.2) and (4.3), we have omitted the restrictions on summations which arise in view of the relation (2.27). Hence a quantity such as $(\Lambda_{ij} - \Omega)^{-1}$ in Eqs. (4.2) and (4.3) should be understood as $(\Lambda_{ij} - \Omega)^{-1}$ with $i \neq j$. It may be noted that the frequencies Ω_1 and Ω_2 in Eqs. (4.1)–(4.3) stand for the sums of frequencies $\omega_1 + \omega_a$ and $\omega_2 + \omega_b$, respectively, with ω_1, ω_2 (ω_a, ω_b) being the Fourier components of the weak field (dipole-moment operator in the dressed-state basis).

In contrast to the case of linear response, the second-order response $R^{(2)}$ consists of two different types of contributions given, respectively, by Eqs. (4.2) and (4.3). The first contribution depends entirely on the relaxation of the off-diagonal elements of the density operator in the dressed-state picture $\tilde{\rho}$, as in the case of the linear response. However, the second contribution depends, in addition, on the relaxation of the diagonal elements as well through the matrix elements of B [Eq. (2.28)]. Further, it also depends on the diagonal elements of the dipole-moment operator in the dressed-state basis $(\tilde{d}_q^\mu)_{jj}$, which are in general nonzero. We next discuss how each term in the expansion of $R^{(2)}$ can be represented by a diagram. For this purpose we will use double-sided diagrams of the type used in the past [26–33] but now the interpretation will be different. We follow the convention used by Prior [31] in writing the double-sided diagrams. In addition we will need an additional type of double-sided diagrams as shown below.

A. Basic features of the diagrammatic method

A double-sided diagram consists of two parallel lines with time advancing upward. The two lines correspond to the evolution of the ket and the bra parts of the initial vector $|\tilde{i}\rangle \langle \tilde{i}|$. It may be noted that $|\tilde{i}\rangle \langle \tilde{i}|$ is a “vector” in the Liouville space, i.e., the space obtained by taking the direct product of two Hilbert spaces each of which is spanned by the basis vectors $|\tilde{i}\rangle$. The diagrammatic method involves keeping track of the successive evolution of the initial vector $|\tilde{i}\rangle \langle \tilde{i}|$ into other vectors in the Liou-

ville space as a result of the interaction of the system with the weak fields in the presence of the strong fields, and as a result of the relaxation of the system in the presence of strong fields. The interactions with the weak fields are represented by wavy arrows placed on the two sides of the diagram. The bra and ket vectors are suitably placed alongside the two parallel lines so that a wavy line drawn, say above $|\tilde{i}\rangle$ and below $|\tilde{k}\rangle$ on the ket side indicates the transformation of $|\tilde{i}\rangle$ into $|\tilde{k}\rangle$. A wavy line pointing upward (downward) represents absorption (emission) of a photon of the weak field in presence of the strong field.

The rules for the diagrams follow from the analytical structure of the nonlinear response (3.3). We examine the generation at the frequency $\omega_q + \sum_{i=1}^n \Omega_i$. A term corresponding to a given double-sided diagram consists of three factors, as follows.

(1a) An initial density-matrix element.

(2a) A product of dipole matrix elements: the rule for writing down these matrix elements follows from the relations given below:

$$L_{aa} |\tilde{k}\rangle \langle \tilde{j}| = -i \sum_m [(\tilde{d}_a^\alpha)_{mk} |\tilde{m}\rangle \langle \tilde{j}| + (-\tilde{d}_a^\alpha)_{jm} |\tilde{k}\rangle \langle \tilde{m}|], \quad (4.4)$$

$$\text{Tr}(\tilde{d}_q^\mu |\tilde{k}\rangle \langle \tilde{j}|) = (\tilde{d}_q^\mu)_{jk}. \quad (4.5)$$

The rule for writing the dipole-matrix elements reads as follows.

One may begin at the ket and the bra parts of the initial vector and trace upwards. On the ket side, the evolution of $|\tilde{k}\rangle$ into $|\tilde{m}\rangle$, for instance, gives rise to a factor $(\tilde{d}_a^\alpha)_{mk}$ in the product of matrix elements, where α is the index corresponding to the vector component of the field. On the bra side, on the other hand, the evolution of $\langle \tilde{j}|$ into $\langle \tilde{m}|$ for instance, gives rise to a factor $(-\tilde{d}_a^\alpha)_{jm}$. The crossing from the bra side to the ket side, say from the bra $\langle \tilde{k}|$ to the ket $|\tilde{j}\rangle$ gives rise to an additional factor $(\tilde{d}_q^\mu)_{jk}$. This additional factor comes from the trace operation as in Eq. (4.5).

(3a) A propagator or a product of propagators: the rule for writing the propagators follows from the relation

$$(iL_0 - \Omega)^{-1} |\tilde{k}\rangle \langle \tilde{j}| = (\Lambda_{kj} - \Omega)^{-1} |\tilde{k}\rangle \langle \tilde{j}|, \quad k \neq j, \quad (4.6)$$

where Λ_{kj} is the complex resonance frequency of the dressed atom as defined by Eq. (2.21b). The rule for writing the propagators reads as follows.

One may advance in time until after an interaction vertex is encountered. If the “vector” at that point is, say, $|\tilde{k}\rangle \langle \tilde{j}|$ ($k \neq j$), then the corresponding propagator is given by $(\Lambda_{kj} - \Omega_r)^{-1}$, where Ω_r is the weighted sum of the photon frequencies appearing below that point, the weighting factor being $+1$ for a photon absorbed and -1 for a photon emitted.

The terms in the first contribution $A^{(2)}$, as they depend on the relaxation of the off-diagonal elements of $\tilde{\rho}$ only, can be represented by the diagrams such as are described above. Here it may be noted that it is not necessary to explicitly indicate such a relaxation in these diagrams. This is due to the simplicity of the relaxation model (3.3) that we have assumed so that the relaxation-dependent propagation operator $(iL_0 - \Omega)^{-1}$ does not transform an off-diagonal element such as $|\tilde{k}\rangle \langle \tilde{j}|$ into some other element but merely scales it by the propagation factor $(\Lambda_{kj} - \Omega_r)^{-1}$. Further, the structure of the off-diagonal propagator is not modified in any nontrivial way due to the relaxation, except for ω_{kj} going to $\omega_{kj} - i\Gamma_{kj} \equiv \Lambda_{ij}$. Here it is superfluous to indicate in the diagrams the transformation of the vector $|\tilde{k}\rangle \langle \tilde{j}|$ into itself. The rules given above can therefore be used to draw the diagrams for the terms in $A^{(2)}$ [Eq. (4.2)]. On the other hand, in order to represent the terms in $B^{(2)}$ [Eq. (4.3)] that arise due to the relaxation of the diagonal elements of the density operator, one needs a different type of diagrams in which the relaxation-induced population transfers among the dressed levels are indicated explicitly. Hence the topology of these diagrams as well as the rules for these diagrams must be substantially different from those for the diagrams of the first type that represent the terms in the first contribution $A^{(2)}$.

First we will consider a typical term in the first contribution $A_{\mu\alpha\beta}^{(2)}$ [Eq. (4.2)], namely,

$$T_1 = \tilde{\rho}_{ii}^{(0)} \frac{(-\tilde{d}_a^\alpha)_{ik} (\tilde{d}_q^\mu)_{kj} (\tilde{d}_b^\beta)_{ji}}{(\Lambda_{ji} - \Omega_2)(\Lambda_{jk} - \Omega_1 - \Omega_2)}, \quad (4.7)$$

and explain how, using the rules (1a)–(3a) given above, one can draw the corresponding diagram. One can see from the structure of the term (4.7) that it represents the evolution of the initial vector $|\tilde{i}\rangle \langle \tilde{i}|$ into $|\tilde{j}\rangle \langle \tilde{i}|$ as a result of the absorption of a photon of frequency Ω_2 , and subsequently into $|\tilde{j}\rangle \langle \tilde{k}|$ as a result of the absorption of another photon of frequency Ω_1 . Thus while the first interaction should be placed on the ket side (since $|\tilde{i}\rangle$ is transformed to $|\tilde{j}\rangle$) the second interaction should be placed on the bra side (since $\langle \tilde{i}|$ is transformed into $\langle \tilde{k}|$). The diagram corresponding to the above term has been drawn in Fig. 1.

There are $2^2 \times 2! = 8$ ways in which two interactions can be placed on two sides of a double-sided diagram in two different time orders. Thus there are eight diagrams of the first type that contribute to $R^{(2)}$ and these are

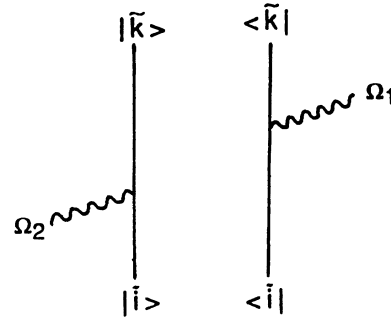


FIG. 1. Diagram representing a typical term in the second-order response.

given in Fig. 2. The corresponding terms are given on the right-hand side of each diagram. These terms add up to give the contribution $A^{(2)}$ [Eq. (4.2)]. It must be noted here that although the $2!$ permutations of the indices $(\Omega_1, \alpha) \leftrightarrow (\Omega_2, \beta)$ in the four terms in the expression (4.2) do not bear a one-to-one correspondence with the $2!$ permutations of the time orders in the diagrams that correspond to these four terms, the two results, in sum, yield the same terms in $A^{(2)}$. This equivalence between the results of the analytic and diagrammatic calculations of the nonlinear response is general and applies to all our further discussion.

B. Population-transfer diagrams

As we have pointed out at the end of Sec. II, the matrix elements of B arise due to the transfers of population among the dressed levels. Thus in order to represent the terms in $B^{(2)}$ [Eq. (4.3)] which involve the matrix elements of B , we must have diagrams that contain the ingredient about such population transfers among the levels concerned. We now describe the topology of these population-transfer diagrams [34] as well as the rules for these diagrams. A population-transfer diagram is, in all respects but one, the same as the usual diagram (the topology of which has been described in detail above). The one important respect in which the population-transfer diagram differs from the usual diagram, as the name indicates, is the additional information that it carries about the transfer of population from one dressed level to another that is brought about by relaxation processes. The transfer of population from, say, level $|\tilde{k}\rangle$ to $|\tilde{j}\rangle$, which in fact corresponds to the evolution of the vector $|\tilde{k}\rangle \langle \tilde{k}|$ to $|\tilde{j}\rangle \langle \tilde{j}|$ in Liouville space, is denoted by means of two double arrows on each of the two parallel lines extending from $|\tilde{k}\rangle$ to $|\tilde{j}\rangle$ on the ket side and from $\langle \tilde{k}|$ to $\langle \tilde{j}|$ on the bra side. We give below the rules for writing the population-transfer diagrams.

The term consists of three factors, as follows.

(1b) An initial density-matrix element.

(2b) A product of dipole-matrix elements. The rule is the same as in (2a) and reads as follows.

One may begin at the ket and the bra parts of the initial vector and trace upwards. On the ket side, the evolu-

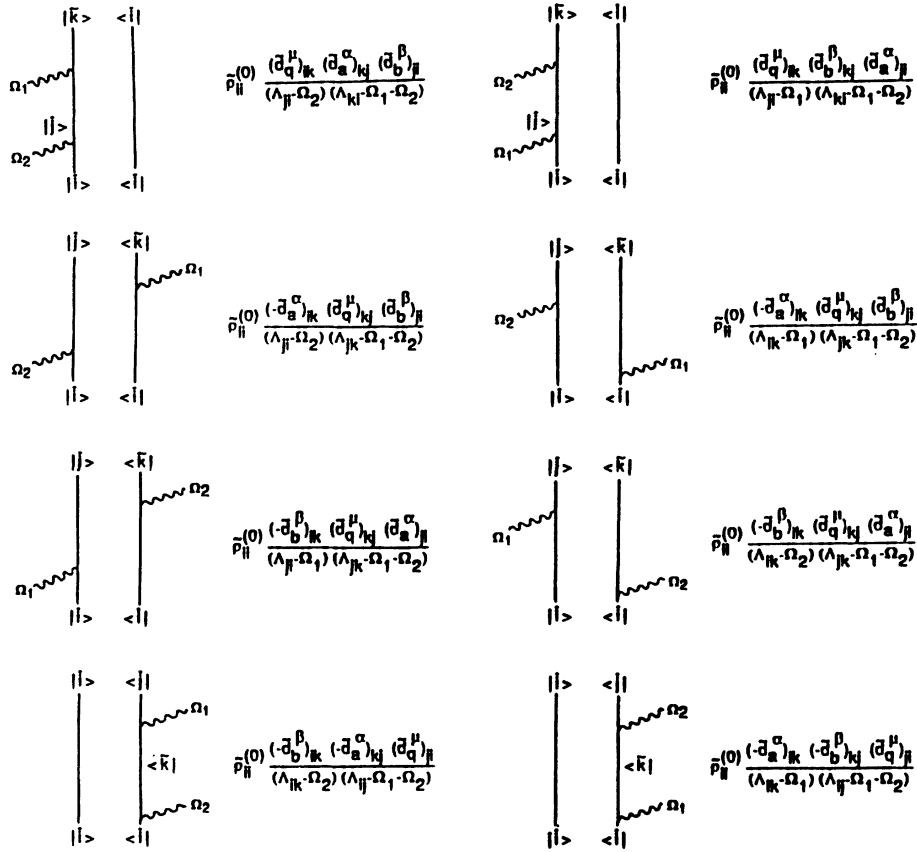


FIG. 2. The eight diagrams of the first type contributing to the second-order response. On the right-hand side of each diagram is the corresponding term.

tion of $|\bar{k}\rangle$ into $|\bar{m}\rangle$, for instance, gives rise to a factor $(\bar{d}_a^\alpha)_{mk}$ in the product of matrix elements, where α is the index corresponding to the Fourier component of the field. On the bra side, on the other hand, the evolution of $\langle \bar{j}|$ into $\langle \bar{m}|$ for instance, gives rise to a factor $(-\bar{d}_a^\alpha)_{jm}$. The additional factor that arises due to the trace operation is $(\bar{d}_q^\mu)_{jk}$, for instance, if the terminal vector is $|\bar{k}\rangle\langle \bar{j}|$.

(3b) A product of propagators: The rules for writing the propagators follow from the relation (3.6) and the relation

$$(iL_0 - \Omega)^{-1} |\bar{k}\rangle\langle \bar{k}| = \sum_j B_{kj}(\Omega) |\bar{j}\rangle\langle \bar{j}|, \quad (4.8)$$

where $B_{kj}(\Omega)$ is defined by the relation (2.28). The rule reads as follows.

One may advance in time until after an interaction vertex is encountered. If the “vector” at that point is, say, $|\bar{k}\rangle\langle \bar{j}|$ ($k \neq j$), then the corresponding propagator is given by $(\Lambda_{kj} - \Omega_r)^{-1}$, while on the other hand if the vector at that point is $|\bar{k}\rangle\langle \bar{k}|$ followed by an evolution to $|\bar{j}\rangle\langle \bar{j}|$ due to a transfer of population from the dressed state $|\bar{k}\rangle$ to $|\bar{j}\rangle$, then the propagator is given by $B_{kj}(\Omega_r)$. Here Ω_r denotes the weighted sum of the photon frequencies appearing below that point, the weighting factor being +1 for a photon absorbed and -1 for a photon emitted.

It may be noted that the rules (1) and (2) are the same for the two types of diagrams. However, the rule (3b) is more general than the rule (3a) in that the former tells us, in addition, about how to write the propagators when there is a relaxation-induced population transfer among the dressed states.

Let us consider now one of the typical terms in the

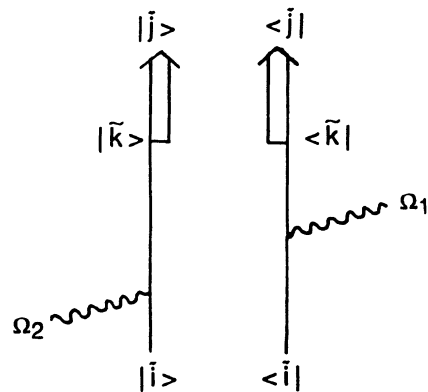


FIG. 3. A population-transfer diagram representing a typical term in the second-order response.

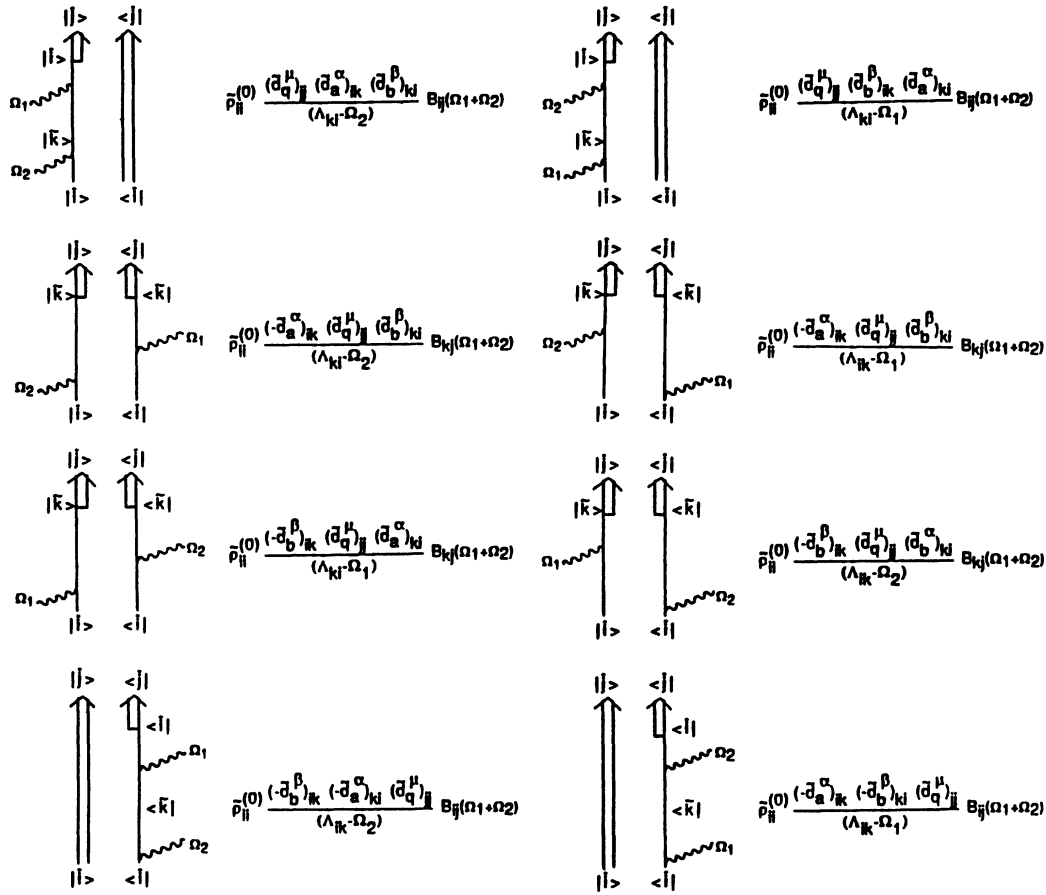


FIG. 4. The eight population-transfer diagrams contributing to the second-order response.

second contribution $B^{(2)}$ [Eq. (4.3)], namely,

$$T_2 = \tilde{\rho}_{ii}^{(0)} \frac{(-\tilde{d}_a^\alpha)_{ik} (\tilde{d}_q^\mu)_{jj} (\tilde{d}_b^\beta)_{ki}}{(\Lambda_{ki} - \Omega_2)} B_{kj}(\Omega_1 + \Omega_2), \quad (4.9)$$

and discuss how the corresponding diagram may be drawn keeping in view the rules (1b)–(3b) given above. It is clear from the structure of the term (4.9) that it represents the evolution of the initial vector $|\tilde{i}\rangle\langle\tilde{i}|$ into $|\tilde{k}\rangle\langle\tilde{i}|$ as a result of the absorption of a photon of frequency Ω_2 , and subsequently into $|\tilde{k}\rangle\langle\tilde{k}|$ as a result of the absorption of another photon of frequency Ω_1 . The fact that the vector at this point is $|\tilde{k}\rangle\langle\tilde{k}|$ implies that the dressed atom, now in the level $|\tilde{k}\rangle$, has the possibility of being transferred, due to relaxation, to another level $|\tilde{j}\rangle$. That this is indeed the case is evident from the presence of the diagonal propagator $B_{kj}(\Omega_1 + \Omega_2)$. Thus the diagram should have the first interaction placed on the ket side (corresponding to the transformation of $|\tilde{i}\rangle$ into $|\tilde{k}\rangle$) and the second interaction on the bra side (corresponding to the transformation of $\langle\tilde{i}|$ into $\langle\tilde{k}|$) and one must draw two double arrows extending from $|\tilde{k}\rangle$ to $|\tilde{j}\rangle$ and from $\langle\tilde{k}|$ to $\langle\tilde{j}|$ on the ket and the bra sides, respectively. It may be noted that a transfer of population from

$|\tilde{k}\rangle$ to $|\tilde{j}\rangle$ takes place after the two photons Ω_1 and Ω_2 have been absorbed so that the argument of the diagonal propagator is $\Omega_1 + \Omega_2$. The diagram corresponding to the term (4.9) has been drawn in Fig. 3.

The eight population-transfer diagrams that contribute to $R^{(2)}$ and the corresponding terms are given in Fig. 4. The contributions from the diagrams in Figs. 3 and 5 add up to give the result (4.1) for the second-order response $R^{(2)}$.

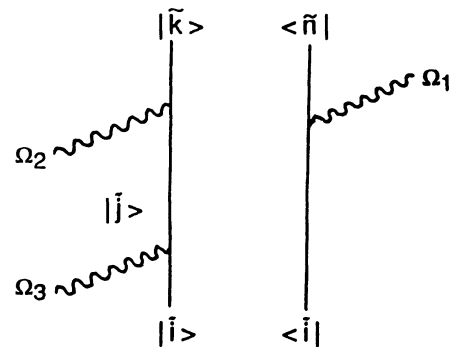


FIG. 5. A diagram belonging to the first class representing a typical term in the third-order response.

V. DIAGRAMMATIC CALCULATION OF THE THIRD-ORDER RESPONSE

In this section we present a diagrammatic calculation of the third-order response $R^{(3)}$ by making use of the

rules for the two types of diagrams, namely, the usual diagrams and the population-transfer diagrams, that we have described in the preceding section.

We first give the analytical expression for $R^{(3)}$ which follows from the general result (2.16):

$$R_{\mu\alpha\beta\gamma}^{(3)}(\omega_q, \Omega_1, \Omega_2, \Omega_3) = \frac{N}{3!} [B_{\mu\alpha\beta\gamma}^{(3)}(\omega_q, \Omega_1, \Omega_2, \Omega_3) + C_{\mu\alpha\beta\gamma}^{(3)}(\omega_q, \Omega_1, \Omega_2, \Omega_3) + D_{\mu\alpha\beta\gamma}^{(3)}(\omega_q, \Omega_1, \Omega_2, \Omega_3)]$$

$$+ \text{five permutations } \begin{bmatrix} \Omega_1 & \Omega_2 & \Omega_3 \\ \alpha & \beta & \gamma \end{bmatrix}$$

$$\rightarrow \begin{bmatrix} \Omega_1 & \Omega_3 & \Omega_2 \\ \alpha & \gamma & \beta \end{bmatrix}, \begin{bmatrix} \Omega_2 & \Omega_1 & \Omega_3 \\ \beta & \alpha & \gamma \end{bmatrix}, \begin{bmatrix} \Omega_2 & \Omega_3 & \Omega_1 \\ \beta & \gamma & \alpha \end{bmatrix}, \begin{bmatrix} \Omega_3 & \Omega_1 & \Omega_2 \\ \gamma & \alpha & \beta \end{bmatrix}, \begin{bmatrix} \Omega_3 & \Omega_2 & \Omega_1 \\ \gamma & \beta & \alpha \end{bmatrix}, \quad (5.1)$$

where the contributions $B^{(3)}$, $C^{(3)}$, and $D^{(3)}$ are given by the expressions

$$B_{\mu\alpha\beta\gamma}^{(3)}(\omega_q, \Omega_1, \Omega_2, \Omega_3) = \sum_{i,n,k,j} \tilde{\rho}_{ii}^{(0)} \left[\frac{(\tilde{d}_q^\mu)_{in}(\tilde{d}_a^\alpha)_{nk}(\tilde{d}_b^\beta)_{kj}(\tilde{d}_c^\gamma)_{ji}}{(\Lambda_{ji} - \Omega_3)(\Lambda_{ki} - \Omega_2 - \Omega_3)(\Lambda_{ni} - \Omega_p)} + \frac{(-\tilde{d}_c^\gamma)_{in}(-\tilde{d}_b^\beta)_{nk}(-\tilde{d}_a^\alpha)_{kj}(\tilde{d}_q^\mu)_{ji}}{(\Lambda_{in} - \Omega_3)(\Lambda_{ik} - \Omega_2 - \Omega_3)(\Lambda_{ij} - \Omega_p)} \right.$$

$$+ \frac{(-\tilde{d}_c^\gamma)_{in}(-\tilde{d}_b^\beta)_{nk}(\tilde{d}_q^\mu)_{kj}(\tilde{d}_a^\alpha)_{ji}}{(\Lambda_{in} - \Omega_3)(\Lambda_{ik} - \Omega_2 - \Omega_3)(\Lambda_{jk} - \Omega_p)} + \frac{(-\tilde{d}_c^\gamma)_{in}(-\tilde{d}_a^\alpha)_{nk}(\tilde{d}_q^\mu)_{kj}(\tilde{d}_b^\beta)_{ji}}{(\Lambda_{in} - \Omega_3)(\Lambda_{jn} - \Omega_2 - \Omega_3)(\Lambda_{jk} - \Omega_p)}$$

$$+ \frac{(-\tilde{d}_b^\beta)_{in}(-\tilde{d}_a^\alpha)_{nk}(\tilde{d}_q^\mu)_{kj}(\tilde{d}_c^\gamma)_{ji}}{(\Lambda_{ji} - \Omega_3)(\Lambda_{jn} - \Omega_2 - \Omega_3)(\Lambda_{jk} - \Omega_p)} + \frac{(-\tilde{d}_c^\gamma)_{in}(\tilde{d}_q^\mu)_{nk}(\tilde{d}_a^\alpha)_{kj}(\tilde{d}_b^\beta)_{ji}}{(\Lambda_{in} - \Omega_3)(\Lambda_{jn} - \Omega_2 - \Omega_3)(\Lambda_{kn} - \Omega_p)}$$

$$\left. + \frac{(-\tilde{d}_b^\beta)_{in}(\tilde{d}_q^\mu)_{nk}(\tilde{d}_a^\alpha)_{kj}(\tilde{d}_c^\gamma)_{ji}}{(\Lambda_{ji} - \Omega_3)(\Lambda_{jn} - \Omega_2 - \Omega_3)(\Lambda_{kn} - \Omega_p)} + \frac{(-\tilde{d}_a^\alpha)_{in}(\tilde{d}_q^\mu)_{nk}(\tilde{d}_b^\beta)_{kj}(\tilde{d}_c^\gamma)_{ji}}{(\Lambda_{ji} - \Omega_3)(\Lambda_{ki} - \Omega_2 - \Omega_3)(\Lambda_{kn} - \Omega_p)} \right], \quad (5.2)$$

$$C_{\mu\alpha\beta\gamma}^{(3)}(\omega_q, \Omega_1, \Omega_2, \Omega_3) = \sum_{i,n,k,j} \tilde{\rho}_{ii}^{(0)} \left[\frac{(\tilde{d}_q^\mu)_{nk}(\tilde{d}_a^\alpha)_{kn}(\tilde{d}_b^\beta)_{ij}(\tilde{d}_c^\gamma)_{ji}}{(\Lambda_{ji} - \Omega_3)(\Lambda_{kn} - \Omega_p)} B_{in}(\Omega_2 + \Omega_3) \right.$$

$$+ \frac{(-\tilde{d}_c^\gamma)_{ij}(-\tilde{d}_b^\beta)_{ji}(-\tilde{d}_a^\alpha)_{kn}(\tilde{d}_q^\mu)_{nk}}{(\Lambda_{ji} - \Omega_3)(\Lambda_{kn} - \Omega_p)} B_{ik}(\Omega_2 + \Omega_3) + \frac{(-\tilde{d}_c^\gamma)_{ij}(-\tilde{d}_b^\beta)_{ji}(\tilde{d}_q^\mu)_{nk}(\tilde{d}_a^\alpha)_{kn}}{(\Lambda_{ij} - \Omega_3)(\Lambda_{kn} - \Omega_p)} B_{in}(\Omega_2 + \Omega_3)$$

$$+ \frac{(-\tilde{d}_c^\gamma)_{ij}(-\tilde{d}_a^\alpha)_{kn}(\tilde{d}_q^\mu)_{nk}(\tilde{d}_b^\beta)_{ji}}{(\Lambda_{ij} - \Omega_3)(\Lambda_{kn} - \Omega_p)} B_{jk}(\Omega_2 + \Omega_3) + \frac{(-\tilde{d}_b^\beta)_{ij}(-\tilde{d}_a^\alpha)_{kn}(\tilde{d}_q^\mu)_{nk}(\tilde{d}_c^\gamma)_{ji}}{(\Lambda_{ij} - \Omega_3)(\Lambda_{kn} - \Omega_p)} B_{jk}(\Omega_2 + \Omega_3)$$

$$+ \frac{(-\tilde{d}_c^\gamma)_{ij}(\tilde{d}_q^\mu)_{nk}(\tilde{d}_a^\alpha)_{kn}(\tilde{d}_b^\beta)_{ji}}{(\Lambda_{ij} - \Omega_3)(\Lambda_{kn} - \Omega_p)} B_{jn}(\Omega_2 + \Omega_3) + \frac{(-\tilde{d}_b^\beta)_{ij}(\tilde{d}_q^\mu)_{nk}(\tilde{d}_a^\alpha)_{kn}(\tilde{d}_c^\gamma)_{ji}}{(\Lambda_{ji} - \Omega_3)(\Lambda_{kn} - \Omega_p)} B_{jn}(\Omega_2 + \Omega_3)$$

$$\left. + \frac{(-\tilde{d}_a^\alpha)_{kn}(\tilde{d}_q^\mu)_{nk}(\tilde{d}_b^\beta)_{ij}(\tilde{d}_c^\gamma)_{ij}}{(\Lambda_{ji} - \Omega_3)(\Lambda_{kn} - \Omega_p)} B_{ik}(\Omega_2 + \Omega_3) \right], \quad (5.3)$$

$$D_{\mu\alpha\beta\gamma}^{(3)}(\omega_q, \Omega_1, \Omega_2, \Omega_3) = \sum_{i,n,k,j} \tilde{\rho}_{ii}^{(0)} \left[\frac{(\tilde{d}_q^\mu)_{nn}(\tilde{d}_a^\alpha)_{ik}(\tilde{d}_b^\beta)_{kj}(\tilde{d}_c^\gamma)_{ji}}{(\Lambda_{ji} - \Omega_3)(\Lambda_{ki} - \Omega_2 - \Omega_3)} B_{in}(\Omega_p) + \frac{(-\tilde{d}_c^\gamma)_{ik}(-\tilde{d}_b^\beta)_{kj}(-\tilde{d}_a^\alpha)_{ji}(\tilde{d}_q^\mu)_{nn}}{(\Lambda_{ik} - \Omega_3)(\Lambda_{ij} - \Omega_2 - \Omega_3)} B_{in}(\Omega_p) \right.$$

$$+ \frac{(-\tilde{d}_c^\gamma)_{ik}(-\tilde{d}_b^\beta)_{kj}(\tilde{d}_q^\mu)_{nn}(\tilde{d}_a^\alpha)_{ji}}{(\Lambda_{ik} - \Omega_3)(\Lambda_{ij} - \Omega_2 - \Omega_3)} B_{jn}(\Omega_p) + \frac{(-\tilde{d}_c^\gamma)_{ik}(-\tilde{d}_a^\alpha)_{kj}(\tilde{d}_q^\mu)_{nn}(\tilde{d}_b^\beta)_{ji}}{(\Lambda_{ik} - \Omega_3)(\Lambda_{jk} - \Omega_2 - \Omega_3)} B_{jn}(\Omega_p)$$

$$+ \frac{(-\tilde{d}_b^\beta)_{ik}(-\tilde{d}_a^\alpha)_{kj}(\tilde{d}_q^\mu)_{nn}(\tilde{d}_c^\gamma)_{ji}}{(\Lambda_{ji} - \Omega_3)(\Lambda_{jk} - \Omega_2 - \Omega_3)} B_{jn}(\Omega_p) + \frac{(-\tilde{d}_c^\gamma)_{ik}(\tilde{d}_q^\mu)_{nn}(\tilde{d}_a^\alpha)_{kj}(\tilde{d}_b^\beta)_{ji}}{(\Lambda_{ik} - \Omega_3)(\Lambda_{jk} - \Omega_2 - \Omega_3)} B_{kn}(\Omega_p)$$

$$\left. + \frac{(-\tilde{d}_b^\beta)_{ik}(\tilde{d}_q^\mu)_{nn}(\tilde{d}_a^\alpha)_{kj}(\tilde{d}_c^\gamma)_{ji}}{(\Lambda_{ji} - \Omega_3)(\Lambda_{jk} - \Omega_2 - \Omega_3)} B_{kn}(\Omega_p) + \frac{(-\tilde{d}_a^\alpha)_{ik}(\tilde{d}_q^\mu)_{nn}(\tilde{d}_b^\beta)_{kj}(\tilde{d}_c^\gamma)_{ji}}{(\Lambda_{ji} - \Omega_3)(\Lambda_{ki} - \Omega_2 - \Omega_3)} B_{kn}(\Omega_p) \right]. \quad (5.4)$$

In Eqs. (5.2)–(5.4), we have used the symbol Ω_p to denote the sum of the frequencies Ω_1 , Ω_2 , and Ω_3 , i.e., $\Omega_p = \Omega_1 + \Omega_2 + \Omega_3$.

The contribution $B^{(3)}$ depends only on the relaxation of the off-diagonal elements of the density operator $\tilde{\rho}$ [35]. Hence the terms in $B^{(3)}$ can be represented by the usual diagrams for which the rules (1a)–(3a) given in Sec. III apply. The contribution $C^{(3)}$, however, depends, in addition, on the population transfers among the dressed levels. Hence the terms in $C^{(3)}$ have to be represented by the population-transfer diagrams described in Sec. IV for which the rules (1b)–(3b) apply. The contribution $D^{(3)}$, on the other hand, depends not only on the relaxation of the off-diagonal elements of $\tilde{\rho}$ and on the population transfers among the dressed levels but it also depends on the nonvanishing of the diagonal elements of the dipole-moment operator in the dressed-state basis. As we have noted earlier, the diagonal elements of the dipole-moment operator in the dressed-state basis are in general nonzero. This is in contrast to the case when the strong fields are absent where the contribution $D^{(3)}$ is nonvanishing only if the system has a permanent dipole moment. The terms in $D^{(3)}$ again are represented by the population-transfer

diagrams. However, these latter diagrams are essentially of a different class due to their being significantly distinct from the diagrams corresponding to the terms in $C^{(3)}$. Thus, in general, we have three classes of diagrams, namely, (i) the diagrams which involve the relaxation of the off-diagonal elements of the density operator alone (although such a relaxation is not explicitly indicated in the diagrams), (ii) the diagrams which involve relaxation-induced population transfers among the dressed levels, and (iii) the diagrams which depend on the nonvanishing of the diagonal matrix elements of the dipole-moment operator in the dressed-state basis. These three classes of diagrams are typified, respectively, by the diagrams corresponding to the three contributions to the third-order response, namely, $B^{(3)}$, $C^{(3)}$, and $D^{(3)}$. It may be noted that the diagrams corresponding to the terms in the contribution $B^{(2)}$ [Eq. (4.3)] in the second-order response belong to both the second as well as the third classes while the diagrams corresponding to the terms in the contribution $A^{(2)}$ [Eq. (4.2)] belong to the first class. In what follows we select a typical term from each of the above three contributions $B^{(3)}$, $C^{(3)}$, and $D^{(3)}$ and illustrate the application of the rules for writing the diagrams.

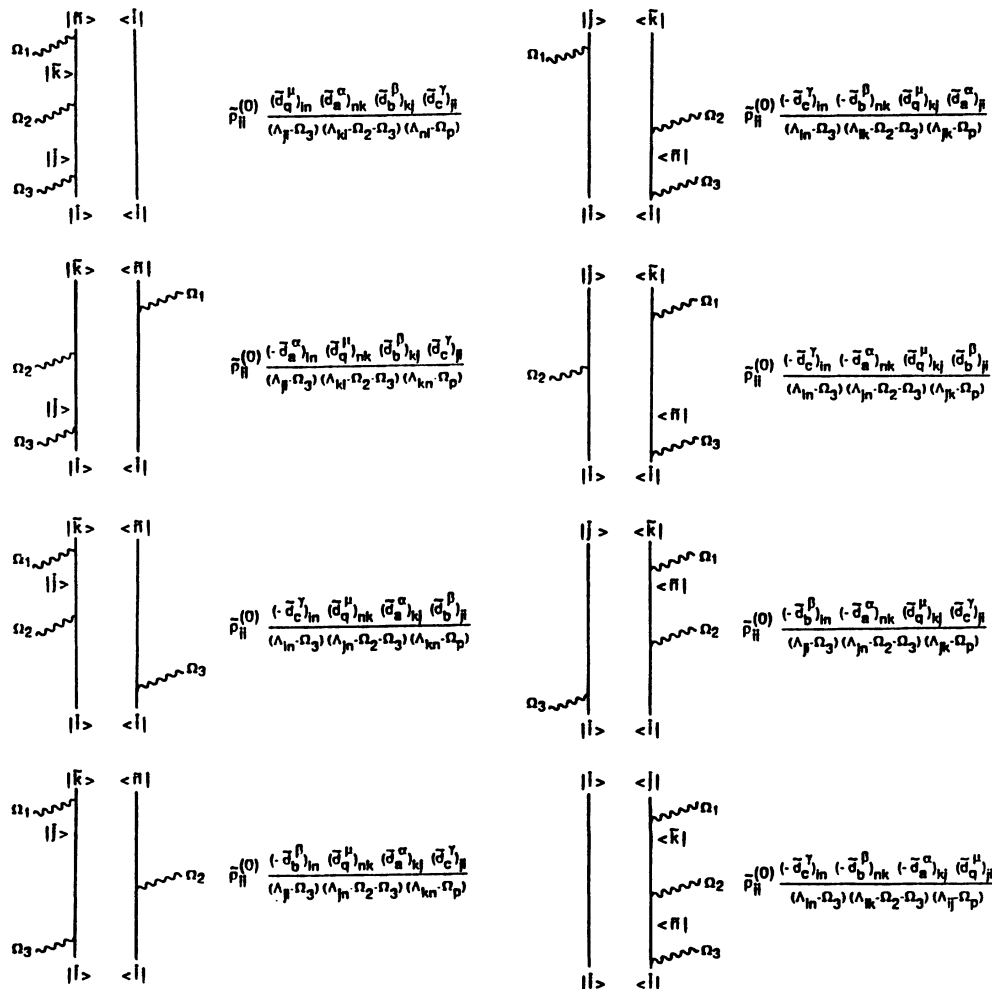


FIG. 6. The eight basic diagrams belonging to the first class that contribute to the third-order response.

Let us consider first a typical term in $B^{(3)}$, namely,

$$T_1 = \bar{\rho}_{ii}^0 \frac{(-\bar{d}_a^\alpha)_{in} (\bar{d}_q^\mu)_{nk} (\bar{d}_b^\beta)_{kj} (\bar{d}_c^\gamma)_{ji}}{(\Lambda_{ji} - \Omega_3)(\Lambda_{ki} - \Omega_2 - \Omega_3)(\Lambda_{kn} - \Omega_p)} \quad (5.5)$$

This term represents the evolution of the initial vector $|\tilde{i}\rangle\langle\tilde{i}|$ into $|\tilde{j}\rangle\langle\tilde{i}|$ and then into $|\tilde{k}\rangle\langle\tilde{i}|$ and then into $|\tilde{k}\rangle\langle\tilde{n}|$ due to the successive absorption of photons Ω_1 , Ω_2 , and Ω_3 , respectively. While the first two interactions (transformation of $|\tilde{i}\rangle$ into $|\tilde{j}\rangle$ and of $|\tilde{j}\rangle$ into $|\tilde{k}\rangle$) are on the ket side the last interaction (transformation of $\langle\tilde{i}|$ into $\langle\tilde{n}|$) is on the bra side. Thus the term (5.5) can be represented by a diagram as in Fig. 5. There are $2^2 \times 3! = 48$ different ways in which three interactions can be placed on two sides of the diagram in six different time orders. We have given in Fig. 6 the eight diagrams corresponding to the eight terms in $A^{(3)}$. The 48 diagrams can be obtained from these eight basic diagrams by permuting the time orders of the three interactions in each of the diagrams. We have demonstrated in Fig. 7 how such a permutation leads to five additional diagrams starting from the basic diagram corresponding to the term given in (5.5). We have also given the corresponding terms, which have been worked out using the rules (1a)–(3a), on the right-hand side of each diagram. The terms corresponding to the 48 diagrams obtained in this manner add up to yield the contribution $B^{(3)}$ to the third-order response.

Let us next consider a typical term in the contribution

$C^{(3)}$, namely, the term given by

$$T_2 = \bar{\rho}_{ii}^0 \frac{(-\bar{d}_a^\alpha)_{kn} (\bar{d}_q^\mu)_{nk} (\bar{d}_b^\beta)_{ij} (\bar{d}_c^\gamma)_{ji}}{(\Lambda_{ji} - \Omega_3)(\Lambda_{kn} - \Omega_p)} B_{ik}(\Omega_2 + \Omega_3) \quad (5.6)$$

This term represents the evolution of the initial vector $|\tilde{i}\rangle\langle\tilde{i}|$ into $|\tilde{j}\rangle\langle\tilde{i}|$ and then into $|\tilde{i}\rangle\langle\tilde{i}|$ due to successive absorption of photons Ω_2 and Ω_3 , respectively. As the structure of the second propagator suggests, a relaxation-induced population transfer occurs at this stage so that $|\tilde{i}\rangle\langle\tilde{i}|$ evolves into $|\tilde{k}\rangle\langle\tilde{k}|$. Finally, $|\tilde{k}\rangle\langle\tilde{k}|$ evolves into $|\tilde{k}\rangle\langle\tilde{n}|$ due to the absorption of the photon Ω_1 . While the first two interactions (transformation of $|\tilde{i}\rangle$ into $|\tilde{j}\rangle$ and of $|\tilde{j}\rangle$ into $|\tilde{i}\rangle$) are on the ket side the last interaction (transformation of $\langle\tilde{k}|$ into $\langle\tilde{n}|$) is on the bra side. Thus the term (5.6) can be represented by a diagram as in Fig. 8. The eight basic diagrams belonging to this class that contribute to the third-order response $R^{(3)}$ are given in Fig. 9 along with the terms corresponding to each of the diagrams, which have been worked out using the rules (1b)–(3b). Starting from these eight diagrams, one can obtain the 48 diagrams belonging to this class by permuting the time orders of the three interactions. It may be noted that in the diagrams in Fig. 9, a relaxation-induced population transfer among the dressed levels occurs after two photons of the weak field

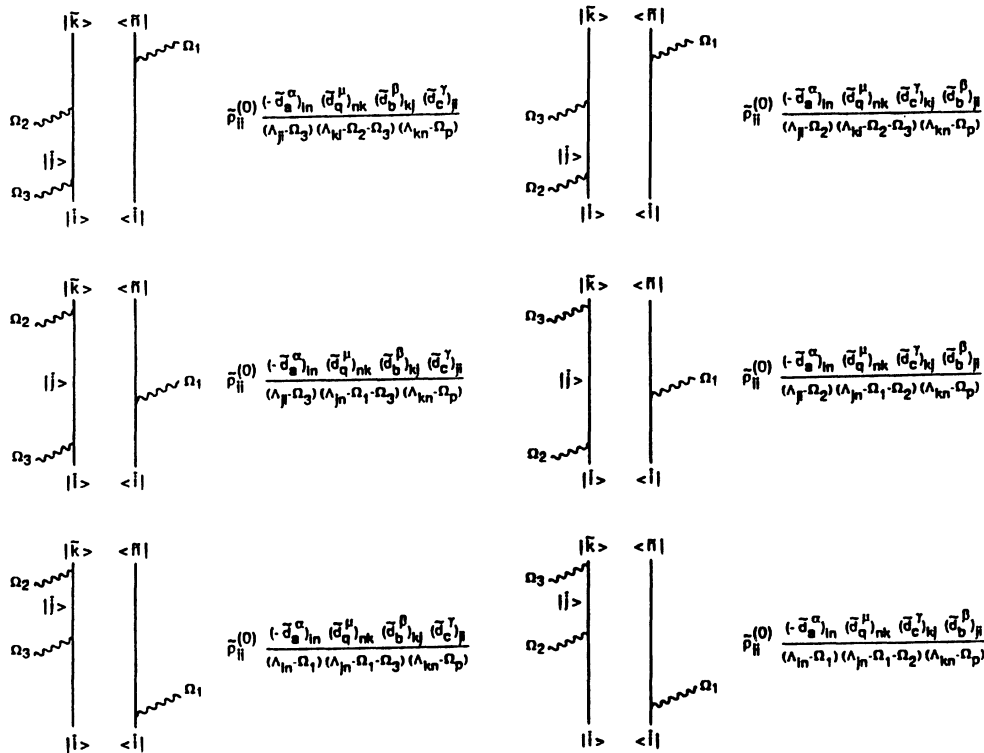


FIG. 7. Six diagrams obtained by permuting the time orders of the three interactions in a typical diagram.

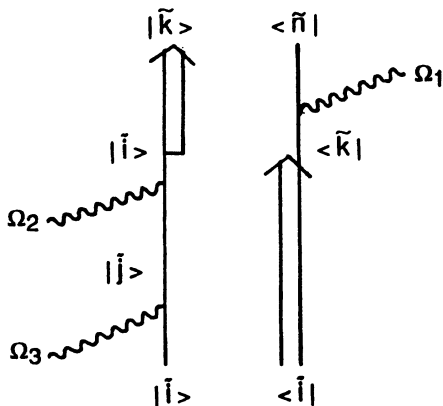


FIG. 8. A diagram belonging to the second class (population-transfer diagram) representing a typical term in the third-order response.

in the presence of the strong field have been absorbed. Hence the two-photon propagator in the terms belonging to these diagrams has the structure $B_{ik}(\Omega_2 + \Omega_3)$.

Finally, let us consider a typical term in the contribution $D^{(3)}$, namely, the term

$$T_3 = \bar{\rho}_{ii}^0 \frac{(-\tilde{d}_a^\alpha)_{ik} (\tilde{d}_q^\mu)_{nn} (\tilde{d}_b^\beta)_{kj} (\tilde{d}_c^\gamma)_{ji}}{(\Lambda_{ji} - \Omega_3)(\Lambda_{ki} - \Omega_2 - \Omega_3)} B_{kn}(\Omega_p). \quad (5.7)$$

This term represents the evolution of the initial vector $|\tilde{i}\rangle \langle \tilde{i}|$ into $|\tilde{j}\rangle \langle \tilde{i}|$ and then into $|\tilde{k}\rangle \langle \tilde{i}|$ and then into $|\tilde{k}\rangle \langle \tilde{k}|$ due to the successive absorption of photons Ω_1 , Ω_2 , and Ω_3 , respectively. At this stage, a relaxation-induced population transfer occurs from the dressed level $|\tilde{k}\rangle$ to $|\tilde{n}\rangle$, as is evident from the structure of the three-photon propagator $B_{kn}(\Omega_p)$. Again while the first two interactions (transformation of $|\tilde{i}\rangle$ into $|\tilde{j}\rangle$ and of $|\tilde{j}\rangle$ into $|\tilde{k}\rangle$) are on the ket side the last interaction (transformation of $|\tilde{i}\rangle$ into $|\tilde{k}\rangle$) is on the bra side. The term (5.7) can be represented by the diagram as in Fig. 10. It may be noted that the structure of the diagram in Fig. 10 is quite different from that in Fig. 8 since in the former, the relaxation-induced population transfer takes place after all the three photons have been absorbed so that the structure of the three-photon propagator is of the type $B_{kn}(\Omega_p)$ ($\Omega_p = \Omega_1 + \Omega_2 + \Omega_3$), while the two-photon prop-

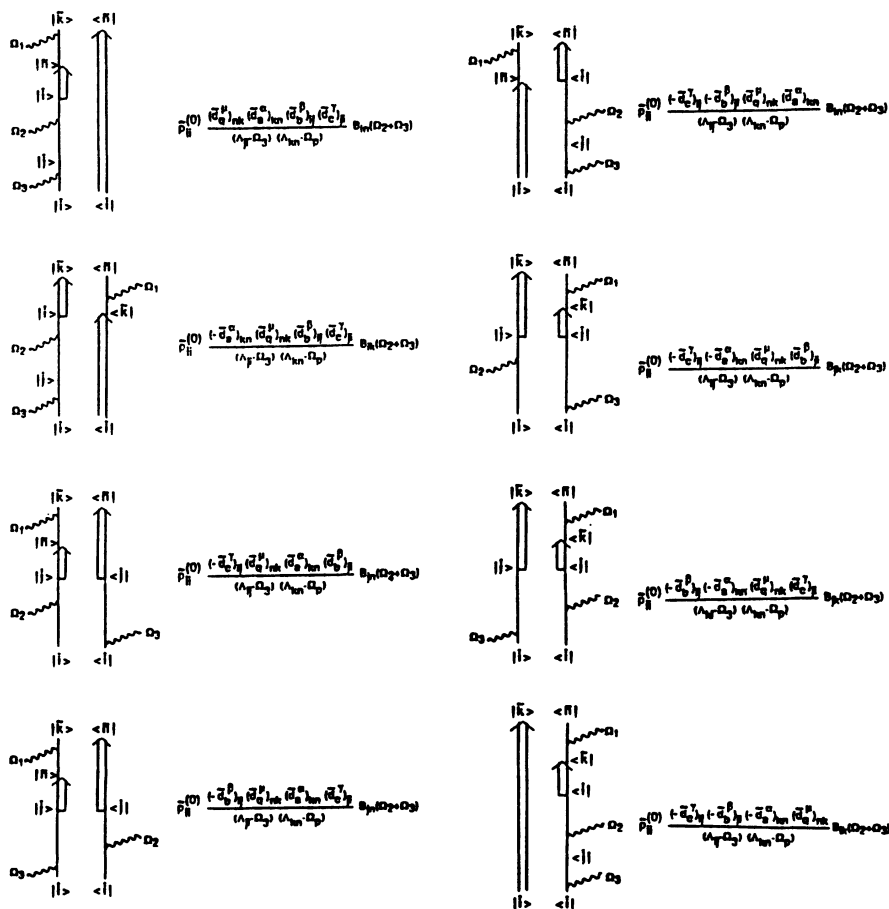


FIG. 9. The eight basic diagrams belonging to the second class that contribute to the third-order response.

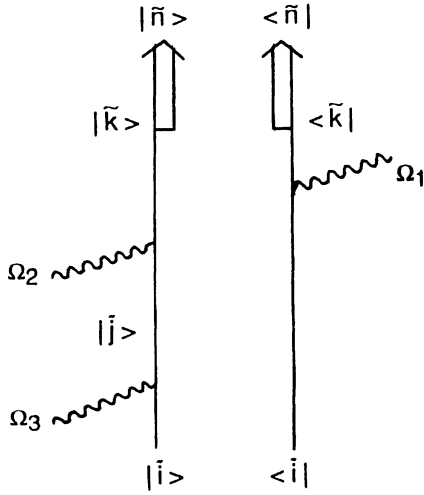


FIG. 10. A diagram belonging to the third class (population-transfer diagram) representing a typical term in the third-order response.

agator has the usual structure $(\Lambda_{ki} - \Omega_2 - \Omega_3)^{-1}$. The eight basic diagrams belonging to this class and the corresponding terms, which have been worked out using the rules (1b)–(3b), are given in Fig. 11. The contribution from the 48 diagrams, derived from these eight basic diagrams by permutation of the time orders of the three interactions, add up to yield the result for $D^{(3)}$ [Eq. (5.4)].

Thus the $48 + 48 + 48 = 144$ diagrams belonging to the three classes discussed above determine the structure of the third-order response $R^{(3)}$ completely. By using the diagrammatic methods developed in the foregoing sections, one can similarly calculate the higher-order response $R^{(n)}$, for $n > 3$ in a straightforward manner.

VI. APPLICATIONS OF THE DIAGRAMMATIC TECHNIQUES

The diagrammatic techniques developed in the foregoing sections can be used to study various phenomena in multilevel systems that arise in the presence of weak probe fields and strong pump fields. We present below some of these applications.

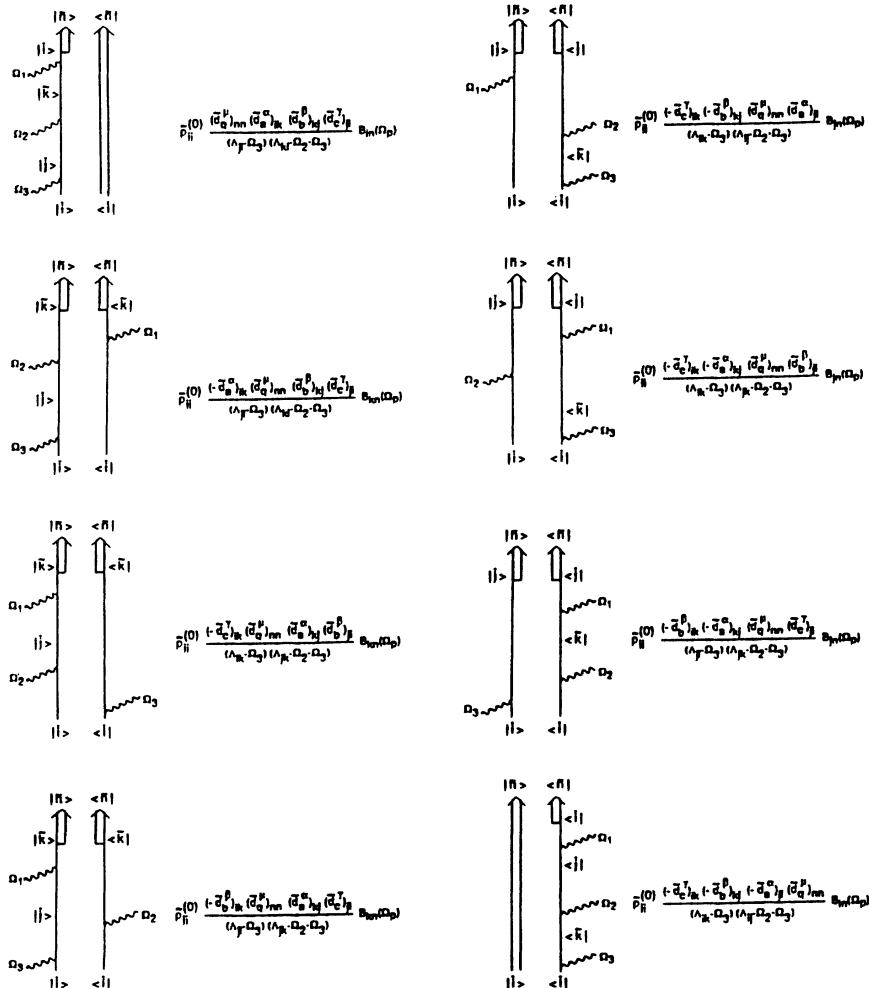


FIG. 11. The eight basic diagrams belonging to the third class that contribute to the third-order response.

A. Resonance at Rabi frequency in absorption

As noted in Sec. III the resonances in the linear response $R^{(1)}$ occur at the transition frequencies of the dressed system. In the case of a two-level system, the energy difference between the dressed states $|\tilde{1}\rangle$ and $|\tilde{2}\rangle$ is equal to the Rabi frequency of the pump field Ω_R . In Fig. 12 we give a typical diagram which describes probe absorption in the presence of a pump. It may be seen from the diagram in Fig. 12 that the lower dressed level $|\tilde{2}\rangle$ is transformed to the upper dressed level $|\tilde{1}\rangle$ due to the absorption of a photon of frequency $\delta = (\omega_s - \omega_l)$. Using the rules (1a)–(3a) we have written down the corresponding term on the right-hand side of the diagram. It is clear from the diagram, as well as from the corresponding term, that resonances at the Rabi frequency occur in probe absorption in the presence of a strong pump [2–5].

B. Resonances at Rabi frequency in four-wave mixing

In Fig. 13 we give a typical diagram which describes the generation of radiation at the frequency $(2\omega_l - \omega_s)$. Here the lower dressed level $|\tilde{2}\rangle$ is transformed to the upper dressed level $|\tilde{1}\rangle$ due to the emission of a photon of frequency $\delta = (\omega_s - \omega_l)$. This process corresponds to the emission of a photon of frequency ω_s in the presence of the pump ω_l . It is clear from the diagram as well as from the corresponding term that resonances at the Rabi frequency occur in four-wave mixing as well [2–5].

C. Resonances at Rabi frequency in fluorescence

The diagrams for the linear response can also be used to study the fluorescence in the presence of a strong pump and a weak probe. In the case of a two-level system the fluorescence intensity will be related to the excited-state population. As explained in Sec. II C the excited-state population $\rho_{11}^{(1)}$ (calculated to first order in the weak field and to all orders in the strong field) can be computed from the linear response $R^{(1)}$ by replacing $\tilde{d}_{\mu q}^{\mu}$ by the operator $S^{-1}|1\rangle\langle 1|S \equiv c_1$. Hence $\rho_{11}^{(1)}$ will then be given by the expression

$$\rho_{11}^{(1)} = \sum_{a,\alpha} \left[\frac{1}{2\pi} \right] \int_{-\infty}^{\infty} d\omega e^{-i\Omega t} \mathcal{N}_{1\alpha}^{(1)}(\Omega) E_{\alpha}(\omega). \quad (6.1)$$

In Figs. 14(a) and 14(b) we have given two diagrams

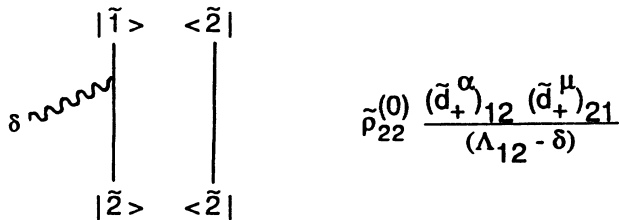


FIG. 12. Typical diagrams for a two-level system interacting with a strong pump and a weak probe. The diagram describes probe absorption. $\delta = (\omega_s - \omega_l)$.

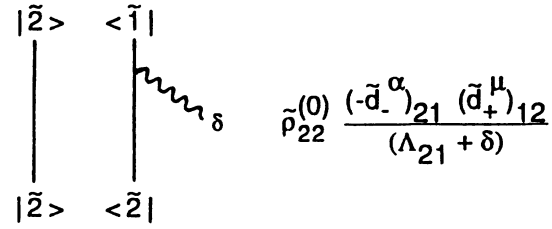


FIG. 13. Same as in Fig. 12 but now the diagram describes four-wave mixing.

(along with the corresponding terms) which contribute to $\mathcal{N}_{1\alpha}^{(1)}(\delta)$ and $\mathcal{N}_{1\alpha}^{(1)}(-\delta)$ ($\delta = \omega_s - \omega_l$), respectively. The excited-state population $\rho_{11}^{(1)}$ will then be given by

$$\rho_{11}^{(1)} = \sum_{\alpha} \tilde{\rho}_{22}^{(0)} [(\tilde{d}_{+}^{\alpha})_{12}(c_1)_{21}(\Lambda_{12} - \delta)^{-1} e^{-i\delta t} (\mathcal{E}_s)_{\alpha} + (\tilde{d}_{-}^{\alpha})_{21}(c_1)_{12}(\Lambda_{21} + \delta)^{-1} e^{i\delta t} (\mathcal{E}_s^*)_{\alpha}], \quad (6.2)$$

$$c_1 = S^{-1}|1\rangle\langle 1|S.$$

There are two more terms that come from the diagrams with the initial vector $|\tilde{1}\rangle\langle \tilde{1}|$. Thus it is clear from the diagrams in Figs. 14(a) and 14(b) that the fluorescence also exhibits resonances at the Rabi frequency.

In the case when an amplitude-modulated field is used instead of the pump and probe fields, the carrier part can be treated as the dressing field and the modulated part as the probe field. In this case, δ will be equal to the modulation frequency Ω_m . Hence, the diagrams such as in Figs. 14 also explain the resonances in modulated fluorescence [25] when the modulation frequency equals the carrier Rabi frequency Ω_R .

D. Subharmonic resonances

Let us consider for simplicity a two-level system interacting with a pump (ω_l) and a probe (ω_s). We consider a typical term in $R_{\mu\alpha\beta}^{(2)}(\omega_l, \delta, \delta)$ $\delta = (\omega_s - \omega_l)$, that is represented by the diagram in Fig. 15(a). This diagram contributes to the second-order response that describes the generation of radiation with frequency $\omega_l + \delta + \delta = 2\omega_s - \omega_l$. It can be seen from the diagram in Fig. 15(a) that the absorption of a single photon of frequency δ as well as the absorption of two photons of frequency δ takes the initial ket $|\tilde{2}\rangle$ (lower dressed level) to the ket $|\tilde{1}\rangle$ (upper dressed level). This implies the existence, in the signal generated with frequency $2\omega_s - \omega_l$, of a resonance at the Rabi frequency ($\delta = \Omega_R$) as well as a resonance at one-half of the Rabi frequency ($2\delta = \Omega_R$), since, as remarked earlier, the energy difference between the dressed levels $|\tilde{1}\rangle$ and $|\tilde{2}\rangle$ is equal to the Rabi frequency of the pump field Ω_R .

Next let us consider a typical term in the third-order response $R_{\mu\alpha\beta\gamma}^{(3)}(\omega_l, \delta, \delta, \delta)$, $\delta = (\omega_s - \omega_l)$, that is represented by the diagram in Fig. 15(b). This diagram describes the generation of radiation with frequency $\omega_l + \delta + \delta + \delta = 3\omega_s - 2\omega_l$. It can be seen from this diagram that the lower ket $|\tilde{2}\rangle$ is transformed to the upper

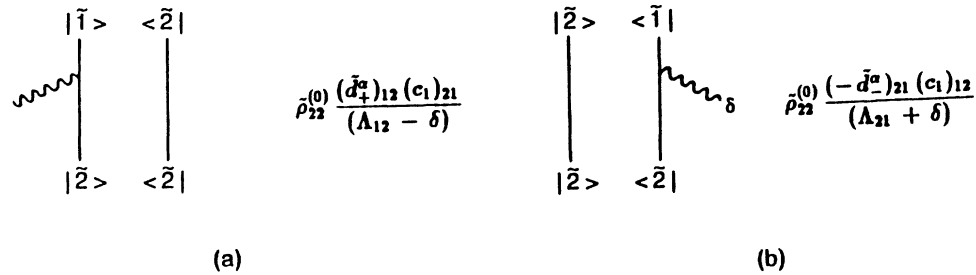


FIG. 14. Diagrams describing fluorescence in presence of a pump and a probe: (a) contribution to $\mathcal{M}_\alpha^{(1)}(\delta)$; (b) contribution to $\mathcal{M}_\alpha^{(1)}(-\delta)$.

ket $|\tilde{1}\rangle$ due to absorption of a single photon, two photons, as well as due to absorption of three photons. This implies the existence of resonances at the Rabi frequency, at one-half of the Rabi frequency, and at one-third of the Rabi frequency in the signal generated with frequency $3\omega_s - 2\omega_l$.

Thus the diagrammatic techniques are useful in analyzing the various subharmonic resonances that occur in various signals that are generated in a system interacting with pump and probe fields.

E. Two-photon gain in a dressed two-level system

There has been considerable interest in recent years in media that exhibit two-photon gain as such media allow for the possibility of two-photon lasing. Lewenstein, Zhu, and Mossberg [15] have shown recently that two-

level atoms dressed by a strong pump exhibit a two-photon gain. This can be understood from the fact that the diagonal elements of the dipole-moment operator in the dressed-state basis are in general nonzero. Hence the nonlinear response that describes the generation of radiation at the probe frequency ω_s , namely, $R^{(3)}(\omega_l, \delta, -\delta, \delta)$, $\delta = (\omega_s - \omega_l)$, exhibits a two-photon resonance at $2\delta = \pm\Omega_R$ (resonance at one-half of the pump Rabi frequency). However, for gain considerations, only the left sideband $\delta < 0$ is of interest. We have given in Fig. 16 some of the diagrams that contribute to $R^{(3)}(\omega_l, \delta, -\delta, \delta)$ along with the corresponding terms. These must be supplemented by diagrams with the initial vector $|\tilde{1}\rangle\langle\tilde{1}|$ which we have not given but which can be easily written down. The contribution from all these diagrams adds up to yield the result

$$R^{(3)}(\omega_l, \delta, -\delta, \delta) = -(\tilde{\rho}_{11}^{(0)} - \tilde{\rho}_{22}^{(0)}) (\tilde{d}_+)_2 (\tilde{d}_-)_1 [(\tilde{d}_+)_1 - (\tilde{d}_+)_2] [(\tilde{d}_-)_1 - (\tilde{d}_-)_2] \\ \times \frac{1}{(\Lambda_{21} - \delta)(\Lambda_{21} - 2\delta)} \left(\frac{1}{(\Lambda_{21} - \delta)} + \frac{1}{\delta + i(p_{12} + p_{21})} \right), \quad (6.3)$$

where p_{12} and p_{21} are, respectively, the rates of decay from lower dressed level $|\tilde{2}\rangle$ to the upper dressed level $|\tilde{1}\rangle$ and vice versa. It may be noted that in writing Eq. (6.3) we have omitted the diagrams that do not yield terms with the two-photon resonant denominator

$(\Lambda_{21} - 2\delta)^{-1} = -(\Omega_R + 2\delta + iq_{12})^{-1}$. Further, assuming a near two-photon resonance condition, we have also omitted the diagrams that yield terms containing one or more antiresonant terms such as, for example $(\Lambda_{12} + \delta)^{-1}$ or $(\Lambda_{12} + 2\delta)^{-1}$. The omission of such antiresonant terms

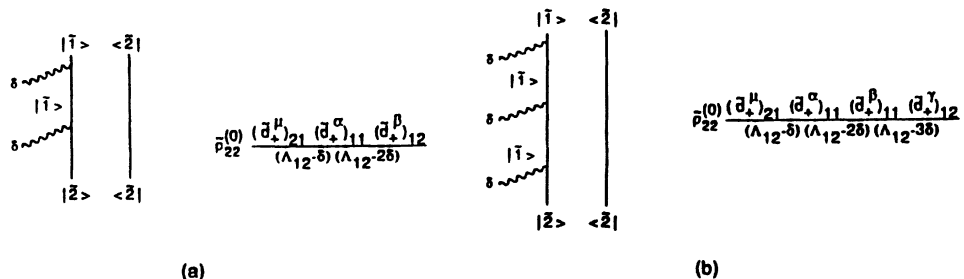


FIG. 15. Typical diagrams describing subharmonic resonances in a two-level system. (a) and (b) correspond to the diagrams contributing to the second-order response and third-order response, respectively.

amounts to a generalized rotating-wave approximation [10] in the modified interaction $F(t)$ [Eq. (2.7b)]. Such a rotating-wave approximation leads to a considerable reduction in the number of diagrams that contribute to any particular nonlinear process. It may be noted that we have for simplicity suppressed the Cartesian indices in writing the dipole-moment matrix elements in Eq. (6.3). The expression in Eq. (6.3) may be compared with the corresponding one for the linear response describing

probe absorption. This follows from Eq. (3.6a) and is given by

$$R^{(1)}(\omega_1, \delta) = -(\bar{\rho}_{11}^{(0)} - \bar{\rho}_{22}^{(0)})(\bar{d}_+)^{12} \times (\bar{d}_-)^{21}(\Lambda_{21} - \delta)^{-1}. \quad (6.4)$$

The dipole-moment matrix elements in Eqs. (6.3) and (6.4) are explicitly given by

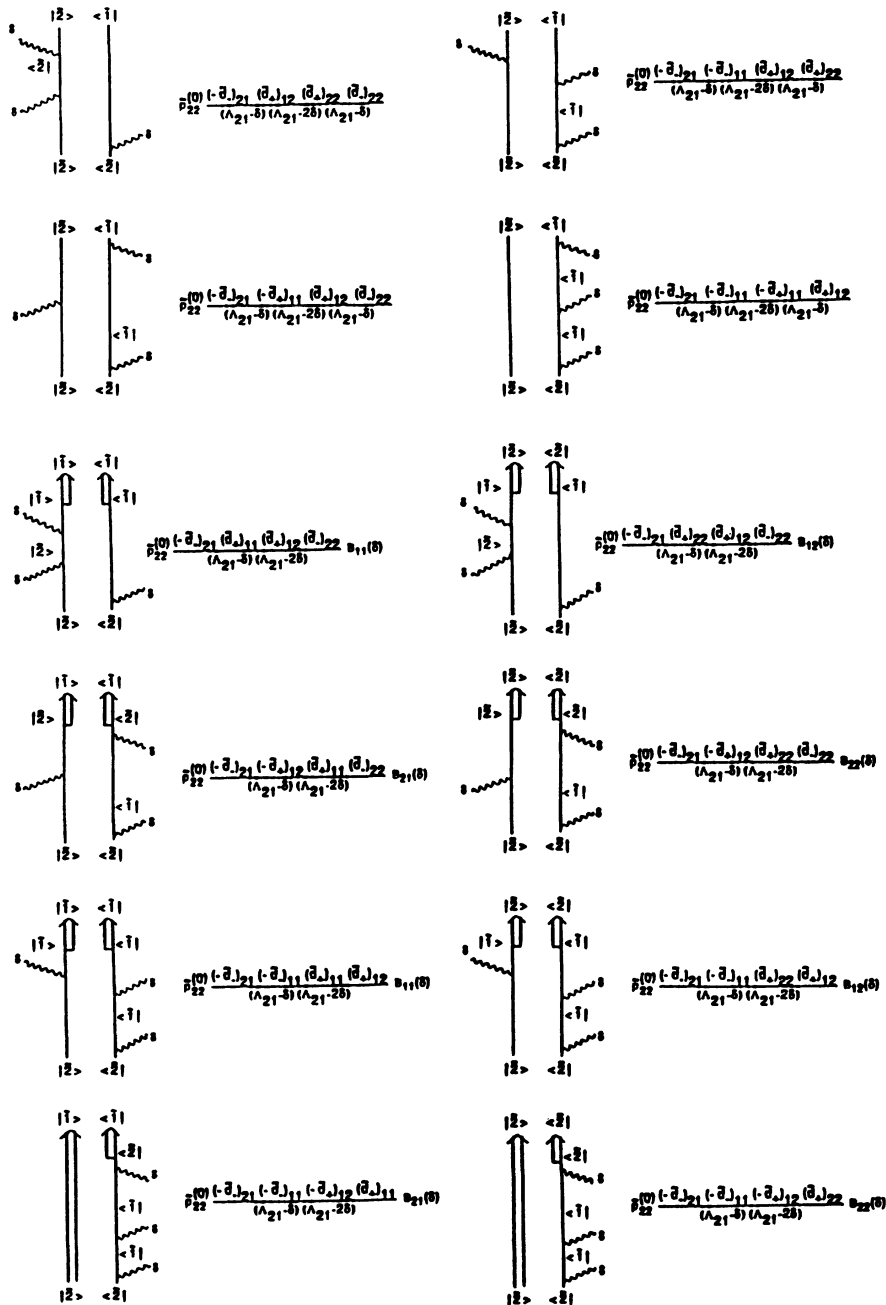


FIG. 16. Diagrams yielding two-photon resonant terms in the third-order response of a dressed two-level system.

$$\begin{aligned}
(\tilde{d}_-)_{12} &= (\tilde{d}_+)_{21} = -d_{12} \sin^2 \phi, \\
(\tilde{d}_-)_{21} &= (\tilde{d}_+)_{12} = d_{12} \cos^2 \phi, \\
(\tilde{d}_-)_{11} &= (\tilde{d}_+)_{11} = -(\tilde{d}_-)_{22} \\
&= -(\tilde{d}_+)_{22} = d_{12} \sin \phi \cos \phi,
\end{aligned} \tag{6.5a}$$

$$\tan 2\phi = \frac{|G|}{\Delta}, \tag{6.5b}$$

where G is the atom-pump coupling coefficient and Δ is the atom-pump detuning. It can be seen from Eq. (6.4) that in general $(\tilde{\rho}_{11}^{(0)} - \tilde{\rho}_{22}^{(0)}) < 0$ and hence the imaginary part of $R^{(1)}(\omega_l, \delta)$ is negative in the neighborhood of the left Rabi sideband $\delta = -\Omega_R$. This gives rise to a linear gain and, as has been demonstrated recently by Lezama *et al.* [16], such a gain is useful for single-photon lasing. On the other hand, in the neighborhood of $\delta = -\Omega_R$ the imaginary part of $R^{(3)}(\omega_l, \delta, -\delta, \delta)$ is positive and hence this acts as a nonlinear loss term in the case of single-photon laser action. However, the imaginary part of $R^{(3)}(\omega_l, \delta, -\delta, \delta)$ is negative in the neighborhood of the subharmonic resonance $2\delta = -\Omega_R$ and hence in this case one has a two-photon gain. It is instructive to look at this result in comparison with the case of a bare two-level atom. It is well known that the nonlinear susceptibility $\chi^{(3)}(\omega_s, -\omega_s, \omega_s)$ of a bare two-level atom exhibits a two-photon resonance $2\omega_s = \omega_{12}$ (where ω_{12} is the transition frequency of the two-level atom) provided the atom has a permanent dipole moment, i.e., the diagonal elements of the dipole-moment operator, namely, d_{11} and d_{22} , are nonzero.

F. dc-field-induced second-harmonic generation

It is a well-known fact that second-harmonic generation cannot take place in systems that have a center of inversion symmetry, for example, in atomic vapors. Usually, a dc field is applied to the system to break the symmetry [20]. The dc field has the effect of mixing the system levels so that the matrix elements of the dipole-moment operator in this mixed basis may be nonvanishing, i.e., $\langle \tilde{i} | d | \tilde{i} \rangle \neq 0$, where the $|\tilde{i}\rangle$ now represent the mixed levels. Thus one has a nonvanishing second-order susceptibility in this case which leads to second-harmonic generation.

The coupling between the dc field and the system may well be quite strong, in which case the dc field may be thought of as “dressing” the system levels. It may be noted that the dressing now is done by a field with zero frequency, i.e., $\omega_l = 0$. Hence in such a case, the second-order response $R^{(2)}(0, \omega_s, \omega_s)$ describes the generation of radiation at the second harmonic $2\omega_s$. For the sake of illustration, we consider a model three-level system with excited levels $|1\rangle$ and $|2\rangle$ ($E_1 > E_2$) to be coupled by a dc field while an optical field ω_s to be near resonant with the transition $|2\rangle \leftrightarrow |3\rangle$, $|3\rangle$ being the ground level. The levels $|2\rangle$ and $|3\rangle$ have a parity opposite to that of level $|1\rangle$. In the dressed-state basis, we have $|\tilde{1}\rangle$ and $|\tilde{2}\rangle$ which are a linear combination of levels $|1\rangle$ and $|2\rangle$ due to dc field coupling and $|\tilde{3}\rangle = |3\rangle$. Since the dressed levels $|\tilde{1}\rangle$ and

$|\tilde{2}\rangle$ do not have definite parities, the matrix elements \tilde{d}_{11} , \tilde{d}_{22} , \tilde{d}_{12} , \tilde{d}_{13} , and \tilde{d}_{23} are all nonvanishing. We give in Figs. 17(a) and 17(b) two typical diagrams which contribute to the second-harmonic signal. These diagrams correspond, respectively, to the terms T_1 and T_2 in $R^{(2)}(0, \omega_s, \omega_s)$ given by

$$T_1 = \tilde{\rho}_{33}^{(0)} \frac{\tilde{d}_{31} \tilde{d}_{11} \tilde{d}_{13}}{(\Lambda_{13} - \omega_s)(\Lambda_{13} - 2\omega_s)}, \tag{6.6a}$$

$$T_2 = \tilde{\rho}_{33}^{(0)} \frac{\tilde{d}_{32} \tilde{d}_{22} \tilde{d}_{23}}{(\Lambda_{23} - \omega_s)(\Lambda_{23} - 2\omega_s)}. \tag{6.6b}$$

Here the dipole-moment matrix elements in the dressed-state basis are given by

$$\begin{aligned}
\tilde{d}_{11} &= -\tilde{d}_{22} = d_{12} \sin 2\theta, \quad \tilde{d}_{12} = d_{12} \cos 2\theta \\
\tilde{d}_{13} &= d_{13} \cos \theta, \quad \tilde{d}_{23} = d_{13} \sin \theta,
\end{aligned} \tag{6.7}$$

where θ is defined by

$$\sin 2\theta = \frac{G}{(\delta^2 + G^2)^{1/2}}, \quad \cos 2\theta = \frac{\delta}{(\delta^2 + G^2)^{1/2}}. \tag{6.8}$$

Assuming a near two-photon resonance condition between the ground level $|\tilde{3}\rangle$ and the excited levels $|\tilde{1}\rangle$ and $|\tilde{2}\rangle$, we can approximate $(\Lambda_{13} - \omega_s)$ and $(\Lambda_{23} - \omega_s)$ by ω_s . The expressions in Eqs. (6.6) can be further simplified by rewriting the two-photon resonant terms as $\Lambda_{13} - 2\omega_s = \Delta + (\delta^2 + G^2)^{1/2} - iq_{13}$ and $\Lambda_{23} - 2\omega_s = \Delta - (\delta^2 + G^2)^{1/2} - iq_{23}$, where 2δ denotes the energy difference between the levels $|1\rangle$ and $|2\rangle$ in the absence of the dc field, G the strength of the dc-field-atom coupling, Δ is the two-photon detuning from the center of the Stark split levels, and q_{13} , and q_{23} are the dc-field-dependent relaxation parameters

$$q_{13} = \frac{1}{2} \gamma_{31} \sin^2 \theta, \quad q_{23} = \frac{1}{2} \gamma_{31} \cos^2 \theta. \tag{6.9}$$

Here γ_{31} denotes the rate of decay from level $|1\rangle$ to level $|3\rangle$. If we assume $\delta/G \ll 1$ (i.e., $\cos^2 \theta \approx \sin^2 \theta \approx \frac{1}{2}$), then we can combine the terms in Eq. (6.6) and write the simple result (cf. Ref. [35])

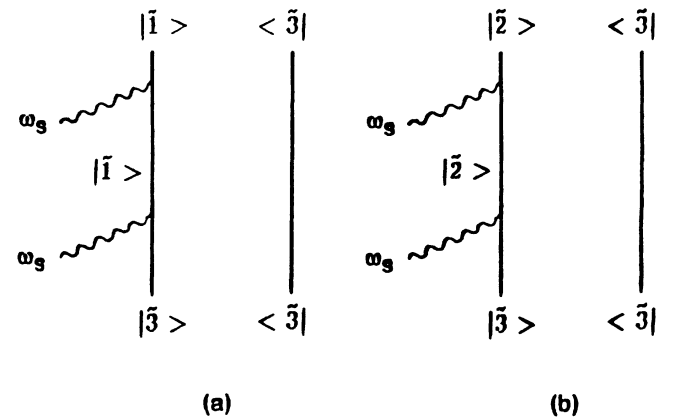


FIG. 17. Two typical diagrams describing dc-field-induced second-harmonic generation in a model three-level system.

$$T = K_2 \left[\frac{1}{\Delta + G - iq} - \frac{1}{\Delta - G - iq} \right], \quad (6.10)$$

where K_2 is a constant factor and we have used q to denote $\gamma_{31}/4$. The two-photon resonant terms in Eq. (6.10) corresponding to the two Stark levels have an opposite sign due to the fact that $\tilde{d}_{11} = -\tilde{d}_{22}$ [Eq. (6.7)]. The intensity of the second-harmonic signal is given by

$$|T|^2 = |K_2|^2 \frac{4G^2}{[(\Delta + G)^2 + q^2][(\Delta - G)^2 + q^2]}. \quad (6.11)$$

It can be seen from Eq. (6.11) that the second-harmonic signal at the two-photon resonance ($\Delta=0$) is a significant fraction of the peak value (i.e., at $\Delta=\pm G$). Hence, as Stoicheff and co-workers [21] have demonstrated, it is possible to have a significantly large second-harmonic signal at the two-photon resonance ($\Delta=0$), at the same time *inducing a transparency in the medium* [36]. Harris and co-workers [22] had earlier shown and recently observed [37] that such a situation where a nonlinear optical process is resonantly enhanced while simultaneously inducing a transparency in the medium can be obtained by applying a strong coupling field between the uppermost state and a level through which the nonlinear process takes place.

It may be noted that we have developed the diagrammatic techniques in this paper for the calculation of the

nonlinear response of a system—the nonlinear response being determined by the mean value of the dipole-moment operator. We would like to remark that the diagrammatic methods can also be used to calculate the two-time correlation functions of the dipole-moment operator. Such two-time correlation functions determine, for example, the spectrum [1] of radiation emitted by an atomic system irradiated by strong external fields. We shall discuss this matter elsewhere.

VII. CONCLUSION

In conclusion, we have developed the diagrammatic methods for the calculation of the nonlinear response of a system that is dressed by resonant pump fields. We have also presented explicit analytical results for the first-, second-, and third-order responses. The rules for the diagrams have been worked out from the formal structure of the nonlinear response. Applications of the diagrammatic techniques to intense-field effects such as subharmonic resonances, dc-field-induced second-harmonic generation, fluorescence, and ionization under laser excitation in the presence of a strong pump and two-photon gain have been discussed.

ACKNOWLEDGMENT

The authors are grateful to the National Science Foundation (U.S.) for supporting this collaborative work.

-
- [1] B. R. Mollow, *Phys. Rev.* **188**, 1969 (1969).
 [2] B. R. Mollow, *Phys. Rev. A* **5**, 2217 (1972).
 [3] R. W. Boyd, M. G. Raymer, P. Narum, and D. J. Harter, *Phys. Rev. A* **24**, 411 (1981); D. J. Harter, P. Narum, M. G. Raymer, and R. W. Boyd, *Phys. Rev. Lett.* **46**, 1192 (1981).
 [4] R. L. Abrams and R. C. Lind, *Opt. Lett.* **2**, 94 (1978); **3**, 205 (1978); T. Y. Fu and M. Sargent, *ibid.* **5**, 433 (1980); G. P. Agrawal, *Phys. Rev. A* **28**, 2286 (1983).
 [5] R. L. Abrams, J. F. Lam, R. C. Lind, D. G. Steel, and P. F. Liao, in *Optical Phase Conjugation*, edited by R. Fisher (Academic, New York, 1983), p. 211.
 [6] G. Grynberg, M. Pinar, and P. Verkerk, *Opt. Commun.* **50**, 261 (1984).
 [7] G. S. Agarwal and S. S. Jha, *J. Phys. B* **12**, 2655 (1979); C. Cohen-Tannoudji and S. Reynaud, *ibid.* **10**, 365 (1977).
 [8] N. Nayak and G. S. Agarwal, *Phys. Rev. A* **31**, 3175 (1985); G. S. Agarwal and N. Nayak, *J. Opt. Soc. Am.* **1**, 164 (1984); G. I. Toptygina and E. E. Fradkin, *Zh. Eksp. Teor. Fiz.* **82**, 429 (1982) [*Sov. Phys.—JETP* **55**, 246 (1982)].
 [9] G. S. Agarwal and N. Nayak, *Phys. Rev. A* **33**, 391 (1986).
 [10] J. H. Eberly and V. D. Popov, *Phys. Rev. A* **37**, 2012 (1988).
 [11] L. W. Hillman, J. Krasinski, R. W. Boyd, and C. R. Stroud, *Phys. Rev. Lett.* **52**, 1605 (1984).
 [12] S. Chakmakjian, K. Koch, and C. R. Stroud, *J. Opt. Soc. Am. B* **5**, 2015 (1988).
 [13] G. S. Agarwal, *J. Opt. Soc. Am. B* **5**, 180 (1988).
 [14] M. Sanjay Kumar and G. S. Agarwal, *Phys. Rev. A* **33**, 1817 (1986).
 [15] M. Lewenstein, Y. Zhu, and T. W. Mossberg, *Phys. Rev. Lett.* **64**, 3131 (1990); Y. Zhu, Q. Wu, S. Morin, and T. W. Mossberg, *ibid.* **65**, 1200 (1990).
 [16] A. Lezama, Y. Zhu, M. Kaskar, and T. W. Mossberg, *Phys. Rev. A* **41**, 1576 (1990).
 [17] G. S. Agarwal, *Phys. Rev. A* **42**, 686 (1990); *Opt. Commun.* **80**, 37 (1990).
 [18] R. Trebino and L. A. Rahn, *Opt. Lett.* **12**, 912 (1987).
 [19] G. S. Agarwal, *Opt. Lett.* **13**, 482 (1988).
 [20] B. J. Dalton and M. Gagen, *J. Phys. B* **18**, 4403 (1985).
 [21] K. Hakuta, L. Marmet, and B. P. Stoicheff, *Phys. Rev. Lett.* **66**, 596 (1991).
 [22] S. E. Harris, J. E. Field, and A. Imamoglu, *Phys. Rev. Lett.* **64**, 1107 (1990).
 [23] C. Cohen-Tannoudji and S. Reynaud, *J. Phys. B* **10**, 345 (1977); **10**, 2311 (1977).
 [24] G. S. Agarwal, *Phys. Rev. A* **19**, 923 (1979).
 [25] R. Saxena and G. S. Agarwal, *J. Phys. B* **13**, 453 (1980).
 [26] S. Y. Yee, T. K. Gustafson, S. A. J. Druet, and J. P. E. Taran, *Opt. Commun.* **23**, 1 (1977).
 [27] S. Y. Yee and T. K. Gustafson, *Phys. Rev. A* **18**, 1597 (1978).
 [28] S. A. J. Druet, B. Attal, T. K. Gustafson, and J. P. E. Taran, *Phys. Rev. A* **18**, 1529 (1978).
 [29] J. Borde and Ch. J. Borde, *J. Mol. Spectrosc.* **78**, 353 (1978).
 [30] S. A. J. Druet and J. P. E. Taran, *Prog. Quantum Elec-*

- tron. **7**, 1 (1982).
- [31] Y. Prior, *IEEE J. Quantum Electron.* **QE-20**, 37 (1984).
- [32] R. Trebino, *Phys. Rev. A* **38**, 2921 (1988).
- [33] R. J. Carlson and J. C. Wright, *Phys. Rev. A* **40**, 5092 (1989).
- [34] In the absence of strong fields, the population-transfer diagrams are important for the calculation of the nonlinear susceptibilities of a system that is undergoing both phase-changing and inelastic collisions [M. Sanjay Kumar, Ph.D. thesis, University of Hyderabad, 1989 (unpublished)].
- [35] In the absence of the strong fields, the contribution $B^{(3)}$ reduces to the expression for the third-order susceptibility derived by Bloembergen *et al.* [see N. Bloembergen, H. Lotem, and R. T. Lynch, Jr., *Indian J. Pure Appl. Phys.* **16**, 151 (1978)].
- [36] Note that in making the secular approximation, the terms of the order of γ/Ω are ignored where γ is a typical relaxation rate and Ω one of the resonance frequencies of the dressed atom. However, situations may arise when the contribution from the secular terms may itself be $\approx \gamma/\Omega$. In such cases the secular approximation should be used with great care. This is indeed the case for the linear response in the region of transparency. Another example where nonsecular terms become important is in connection with lasing without inversion [G. S. Agarwal, *Phys. Rev. A* **44**, 1228 (1991)].
- [37] D. A. King, K. H. Hahn, and S. E. Harris, *Phys. Rev. Lett.* **65**, 2777 (1990).